Eastern-European
JOURNAL
of Enterprise Technologies

Східно-Європейський
ЖУРНАЛ
передових технологій

▪ Applied physics

5/5 (131) 2024

Content

APPLIED PHYSICS

Editorial Team

Information site

Language

English

Українська

Information

For Readers

For Authors

For Librarians

Make a Submission

Open Journal Systems

Collective monographs
with Scopus indexing
from PC TECHNOLOGY CENTER

Offer for scientists from
our partner Scientific Route

How to correctly link to an article in the Eastern European Journal of Enterprise Technologies

Scopus

CiteScore 2022

2.1

SJR 2022

0.283

SNIP 2022

0.514

YouTube

Subscribe

Current Issue

ATOM 1.0

RSS 2.0

RSS 1.0

Visitors

ISSN (print) 1729-3774, ISSN (on-line) 1729-4061

ABSTRACT AND REFERENCES

APPLIED MECHANICS

DOI: 10.15587/1729-4061.2024.314234

OPTIMIZATION OF THE SOLAR CELL BASED ON CADMIUM TELLURIDE BY ADDING THE CdSeTe ABSORBING LAYER (HETEROSTRUCTURE SIMULATION) (p. 6–12)

Hryhorii Ilchuk
Lviv Polytechnic National University, Lviv, Ukraine
ORCID: https://orcid.org/0000-0002-6647-4343

Ihor Semkiv
Lviv Polytechnic National University, Lviv, Ukraine
ORCID: https://orcid.org/0000-0003-3432-8779

Maryana Karkulovska
Lviv Polytechnic National University, Lviv, Ukraine
ORCID: https://orcid.org/0000-0002-1348-6148

Vitalii Vashchynskyi
Lviv Polytechnic National University, Lviv, Ukraine
ORCID: https://orcid.org/0000-0002-6587-6957

Mykola Solovyov
Lviv Polytechnic National University, Lviv, Ukraine
ORCID: https://orcid.org/0000-0001-7678-4049

Cadmium telluride solar cells are among the most common devices for photovoltaic applications. However, the energy conversion efficiency of these elements remains insufficiently high. Using the SCAPS programming environment, research and optimization of a classical thin-film solar cell based on CdTe were carried out. The structure of this element consisted of ITO as a transparent conductive contact, a cadmium sulfide (CdS) layer, and a cadmium telluride (CdTe) absorber layer with a metal contact. To optimize this structure in terms of power conversion efficiency, the influence of the thickness and concentration of acceptor impurities in the CdTe absorbing layer, as well as the influence of the thickness and concentration of donor impurities in the CdS buffer layer, were considered. It was established that the optimal thicknesses for the CdS buffer layer and absorption CdTe layers are 50 nm and 3000 nm, respectively. An additional CdSeTe layer between the CdS and CdTe layers has been proposed as one of the optimization options to improve the device efficiency. The main photovoltaic parameters of such a solar cell were analyzed depending on the thickness of the CdSeTe layer and its selenium content. It has been demonstrated that adding CdSeTe solid solution to the 1500 nm thick CdTe absorber layer increases the efficiency of the solar cell by 6.84 %. The main photovoltaic characteristics of CdS/CdTe and CdS/CdSeTe/CdTe solar cells were compared. The results showed that the simulated CdS/CdSeTe/CdTe structure provides better photoconversion efficiency in the AM1.5G light spectrum compared to the classical CdS/CdTe structure. Such elements can be used to form highly efficient solar panels.

Keywords: solar cell, SCAPS, thin films, heterostructures, cadmium telluride, cadmium chalcogenide.

References

1. Green, M. A., Dunlop, E. D., Hohl-Ebinger, J., Yoshita, M., Kopidakis, N., Hao, X. (2021). Solar cell efficiency tables (Version 58). Progress in Photovoltaics: Research and Applications, 29 (7), 657–667. https://doi.org/10.1002/pip.3444
2. Thompson, N., Ballen, J. (2017). First Solar. MIT Management Sloan School. Available at: https://mitsloan.mit.edu/sites/default/files/2020-03/First%20Solar.IC_.pdf
3. Romeo, A., Artegiani, E. (2021). CdTe-Based Thin Film Solar Cells: Past, Present and Future. Energies, 14 (6), 1684. https://doi.org/10.3390/en14061684
4. Mohamed, H. A. (2015). Optimized conditions for the improvement of thin film CdS/CdTe solar cells. Thin Solid Films, 589, 72–78. https://doi.org/10.1016/j.tsf.2015.04.081
5. Morales-Acevedo, A. (2006). Thin film CdS/CdTe solar cells: Research perspectives. Solar Energy, 80 (6), 675–681. https://doi.org/10.1016/j.solener.2005.10.008
6. Dharmadasa, I. M., Alam, A. E., Ojo, A. A., Echendu, O. K. (2019). Scientific complications and controversies noted in the field of CdS/CdTe thin film solar cells and the way forward for further development. Journal of Materials Science: Materials in Electronics, 30 (23), 20330–20344. https://doi.org/10.1007/s10854-019-02422-6
7. Yang, X., Liu, B., Li, B., Zhang, J., Li, W., Wu, L., Feng, L. (2016). Preparation and characterization of pulsed laser deposited a novel CdS/CdSe composite window layer for CdTe thin film solar cell. Applied Surface Science, 367, 480–484. https://doi.org/10.1016/j.apsusc.2016.01.224
8. Ibrahim, M., Chelvanathan, P., Miraz, M. H., Alkhammash, H. I., Hasan, A. K. M., Akhtaruzzaman, Md. et al. (2022). Comprehensive study on CdSe thin film as potential window layer on CdTe solar cell by SCAPD-1D. Chalcogenide Letters, 19 (1), 33–43. https://doi.org/10.15251/cl.2022.191.33
9. Li, C., Hu, G., Hao, X., Li, C., Tan, B., Wang, Y. et al. (2021). Performance improvement of CdS/CdTe solar cells by incorporation of CdSe layers. Journal of Materials Science: Materials in Electronics, 32 (14), 19083–19094. https://doi.org/10.1007/s10854-021-06425-0
10. Lingg, M., Buecheler, S., Tiwari, A. N. (2019). Review of $CdTe_{1-x}Se_x$ Thin Films in Solar Cell Applications. Coatings, 9 (8), 520. https://doi.org/10.3390/coatings9080520
11. Paudel, N. R., Yan, Y. (2014). Enhancing the photo-currents of CdTe thin-film solar cells in both short and long wavelength regions. Applied Physics Letters, 105 (18). https://doi.org/10.1063/1.4901532
12. Fiducia, T. A. M., Mendis, B. G., Li, K., Grovenor, C. R. M., Munshi, A. H., Barth, K. et al. (2019). Understanding the role of selenium in defect passivation for highly efficient selenium-alloyed cadmium telluride solar cells. Nature Energy, 4 (6), 504–511. https://doi.org/10.1038/s41560-019-0389-z
13. Poplawsky, J. D., Guo, W., Paudel, N., Ng, A., More, K., Leonard, D., Yan, Y. (2016). Structural and compositional dependence of the $CdTe_xSe_{1-x}$ alloy layer photoactivity in CdTe-based solar cells. Nature Communications, 7 (1). https://doi.org/10.1038/ncomms12537
14. Burgelman, M., Nollet, P., Degrave, S. (2000). Modelling polycrystalline semiconductor solar cells. Thin Solid Films, 361-362, 527–532. https://doi.org/10.1016/s0040-6090(99)00825-1
15. Zheng, X., Kuciauskas, D., Moseley, J., Colegrove, E., Albin, D. S., Moutinho, H. et al. (2019). Recombination and bandgap engineering in CdSeTe/CdTe solar cells. APL Materials, 7 (7). https://doi.org/10.1063/1.5098459
16. Doroody, C., Sajedur Rahman, K., Chelvanathan, P., Adib Ibrahim, M., Sopian, K., Amin, N. et al. (2023). Incorporation of Magnesium-doped Zinc Oxide (MZO) HRT Layer in Cadmium Telluride

(CdTe) Solar Cells. Results in Physics, 47, 106337. https://doi.org/10.1016/j.rinp.2023.106337
17. Nykyruy, L. I., Yavorskyi, R. S., Zapukhlyak, Z. R., Wisz, G., Potera, P. (2019). Evaluation of CdS/CdTe thin film solar cells: SCAPS thickness simulation and analysis of optical properties. Optical Materials, 92, 319–329. https://doi.org/10.1016/j.optmat.2019.04.029
18. Bhari, B. Z., Rahman, K. S., Chelvanathan, P., Ibrahim, M. A. (2023). Plausibility of ultrathin CdTe solar cells: probing the beneficial role of MgZnO (MZO) high resistivity transparent (HRT) layer. Journal of Materials Science, 58 (40), 15748–15761. https://doi.org/10.1007/s10853-023-09001-5
19. Filipe, D. I., Chenene, M. L. (2023). Front interface defect signature and benefits of CdSeTe thickness and band gap in CdSeTe/CdTe graded solar cell. https://doi.org/10.21203/rs.3.rs-3462048/v2
20. Zyoud, S. H., Zyoud, A. H., Ahmed, N. M., Abdelkader, A. F. I. (2021). Numerical Modelling Analysis for Carrier Concentration Level Optimization of CdTe Heterojunction Thin Film–Based Solar Cell with Different Non–Toxic Metal Chalcogenide Buffer Layers Replacements: Using SCAPS–1D Software. Crystals, 11 (12), 1454. https://doi.org/10.3390/cryst11121454
21. Liu, X., Abbas, A., Togay, M., Kornienko, V., Greenhalgh, R., Curson, K. et al. (2024). The effect of remnant CdSe layers on the performance of CdSeTe/CdTe photovoltaic devices. Solar Energy Materials and Solar Cells, 267, 112717. https://doi.org/10.1016/j.solmat.2024.112717
22. Munshi, A. H., Kephart, J., Abbas, A., Raguse, J., Beaudry, J.-N., Barth, K. et al. (2018). Polycrystalline CdSeTe/CdTe Absorber Cells With 28 mA/cm^2 Short-Circuit Current. IEEE Journal of Photovoltaics, 8 (1), 310–314. https://doi.org/10.1109/jphotov.2017.2775139

DOI: 10.15587/1729-4061.2024.313878

ASSESSING THE POTENTIAL ACCURACY OF A SMALL-SIZED GONIOMETER WITH EXTENDED DYNAMIC RANGE BASED ON NUCLEAR MAGNETIC RESONANCE (p. 13–25)

Sergiy Ivanov
State University of Information and Communication Technologies, Kyiv, Ukraine
ORCID: http://orcid.org/0000-0003-3001-2451

This paper evaluates potential accuracy characteristics of a small-sized goniometer based on nuclear magnetic resonance with an extended dynamic range. This required constructing a model of goniometer errors, estimating its accuracy based on this model, and formulating practical recommendations for the design of such a device based on the accuracy assessment.

To evaluate the accuracy of a nuclear goniometer, a theoretical model was built that makes it possible to determine the optimal operating parameters of the cell gas mixture, the ranges of their permissible changes, the sensitivity of the goniometer, and the dependence of its characteristics on external and internal factors. In particular, the dependence of output signal of the device on the parameters of gas mixture and optical pumping has been determined. For a goniometer with a cell volume of 8 cm^3, the optimum temperature is 130 °C, and the optimum intensity of the pumping radiation is 5 mW.

The dependence of output signal on the measured angle of rotation was also established, as well as the noise and error dependence of the device on the permissible values of its parameters. Based on the model built, parameters of a goniometer with a cell volume of 8 cm^3 were determined; the maximum angular sensitivity of such a goniometer with complete suppression of technical noise is $\delta\varphi_{sen}$=1.0 arcsec. The greatest contribution to the angle measurement error is from the instability of pumping power I_p ($\Delta I_p/I_p$=0.05) – 85 %, magnetic field B_0 ($\Delta B_0/B_0$=10^{-8}) – 13 %, temperature T ($\Delta T/T$=0.1) – 2 %.

The goniometer under consideration corresponds to the medium accuracy class, $\delta\varphi_{tot}\geq$10 arcsec. It could be used in optical manufacturing for operational control, calibration, and certification of optical products. To improve the angular accuracy of the goniometer, it is necessary to increase the stability of the laser pumping intensity.

Keywords: goniometer, nuclear magnetic resonance, gas cell, optical pumping, Helmholtz coil, Larmor frequency.

References

1. Zheng, L., Tang, Q., Ma, X., Zhang, Y. (1996). High-precision static and dynamic angular measurements with a ring laser gyroю Automated Optical Inspection for Industry, 2899, 50–53. https://doi.org/10.1117/12.253053
2. Pisani, M., Astrua, M., Santiano, M., Beverini, N., Di Virgilio, A., Maccioni, E. et al. (2018). G-LAS: a ring laser gyroscope for high accuracy angle measurements. Journal of Physics: Conference Series, 1065, 032009. https://doi.org/10.1088/1742-6596/1065/3/032009
3. Wie, Z., Yao, H., Ke, L., Jin, Z., Zi, X. (2022). Calibration and Measurement Method of Laser Gyro Goniometer. Metrology Science and Technology, 66 (4), 40–47.
4. Cherepanska, I. Yu., Bezvesilna, O. M., Sazonov, A. Yu. (2019). Precise Intelligent Goniometric System. Visnyk of Vinnytsia Politechnical Institute, 143 (2), 7–14. https://doi.org/10.31649/1997-9266-2019-143-2-7-14
5. Zou, W., Huang, Y., Lin, H., Xue, Z. (2024). New Application and Research of Ring Laser Gyroscope in the Field of Angle Metrology. IEEE Transactions on Instrumentation and Measurement, 73, 1–12. https://doi.org/10.1109/tim.2024.3449940
6. Mou, J., Pang, B., Huang, T., Ying, G., Shu, X. (2019). A new method to eliminate the misalignment angle in dynamic goniometer based on fiber optic gyro. Optik, 193, 162998. https://doi.org/10.1016/j.ijleo.2019.162998
7. Pang, B., Ying, G., Xue, F., Huang, T., Che, S., Shu, X., Mou, J. (2019). Uncertainty analysis of dynamic goniometer based on fiber optic gyroscope. 9th International Symposium on Advanced Optical Manufacturing and Testing Technologies: Optical Test, Measurement Technology, and Equipment, 20, 115. https://doi.org/10.1117/12.2509290
8. Ivanov, S. V. (2016). Porivnialnyi analiz efektyvnosti vydiv namotky volokna chutlyvoho elementa volokonno-optychnoho hiroskopa v umovakh zminy temperatury. Naukovi visti natsionalnoho tekhnichnoho universytetu Ukrainy «Kyivskyi politekhnichnyi instytut», 1, 99–106.
9. Ivanov, S. V., Muravov, V. V., Oliinyk, P. B. (2024). Pat. No. 156304 UA. Honiometr. MPK G01B11/26; No. u202305588; declareted: 21.11.2023; published: 05.06.2024, Bul. No. 23.
10. Skinner, J. G., Ranta, K., Whiting, N., Coffey, A. M., Nikolaou, P., Rosen, M. S. et al. (2020). High Xe density, high photon flux, stopped-flow spin-exchange optical pumping: Simulations versus experiments. Journal of Magnetic Resonance, 312, 106686. https://doi.org/10.1016/j.jmr.2020.106686
11. Cates, G. D., Fitzgerald, R. J., Barton, A. S., Bogorad, P., Gatzke, M., Newbury, N. R., Saam, B. (1992). Rb–129Xe spin-exchange rates due to binary and three-body collisions at high Xe pressures. Physical Review A, 45 (7), 4631–4639. https://doi.org/10.1103/physreva.45.4631

12. Li, R., Quan, W., Fang, J. (2017). Polarization Measurement of Cs Using the Pump Laser Beam. IEEE Photonics Journal, 9 (6), 1–8. https://doi.org/10.1109/jphot.2017.2761779

DOI: 10.15587/1729-4061.2024.310360

DEVELOPMENT OF METHODS FOR MONITORING AND OPTIMIZATION OF UNDERGROUND DRAINAGE SYSTEMS USING WIRELESS SENSOR NETWORKS AND ULTRA-WIDEBAND ANTENNAS (p. 26–36)

Kabi Yelikbay
ALT University, Almaty, Republic of Kazakhstan
ORCID: https://orcid.org/0009-0009-3657-1407

Pramod Kumar
CMR Engineering College, Seethariguda, Telangana, India
ORCID: https://orcid.org/0000-0003-2810-2765

Ruslan Kassym
ALT University, Almaty, Republic of Kazakhstan
University of Jaén, Jaén, Spain
ORCID: https://orcid.org/0000-0001-8024-5224

Tansaule Serikov
S. Seifullin Kazakh Agrotechnical Research University, Astana, Republic of Kazakhstan
ORCID: https://orcid.org/0000-0001-7026-7702

Maxat Orunbekov
ALT University, Almaty, Republic of Kazakhstan
ORCID: https://orcid.org/0000-0002-0220-4053

Ayinuer Turdy
ALT University, Almaty, Republic of Kazakhstan
ORCID: https://orcid.org/0009-0008-1809-9340

Marzhan Temirbekova
ALT University, Almaty, Republic of Kazakhstan
ORCID: https://orcid.org/0000-0003-1911-289X

Arai Tolegenova
S. Seifullin Kazakh Agrotechnical Research University, Astana, Republic of Kazakhstan
ORCID: https://orcid.org/0000-0001-6318-8328

Akmaral Tlenshiyeva
ALT University, Almaty, Republic of Kazakhstan
ORCID: https://orcid.org/0000-0001-8105-1632

Makbal Kassymova
S. Seifullin Kazakh Agrotechnical Research University, Astana, Republic of Kazakhstan
ORCID: https://orcid.org/0009-0009-0299-8816

This research focuses on optimizing ultra-wideband (UWB) antennas, which are critical in modern communication systems due to their wide frequency range (3.1–10.6 GHz) and high data transmission capabilities. The study addresses the challenge of optimizing key antenna parameters – such as return loss, peak gain, and radiation efficiency – while also ensuring energy efficiency and network longevity. Traditional optimization methods, such as LEACH-C, often fail to balance these factors, leading to suboptimal performance.

To solve this problem, the researchers developed the Generalized Position-based Optimization Neural Network (GPON) for UWB antenna optimization. They also evaluated the Position-based Hybrid Neural Network (PAN) method, comparing its performance with existing algorithms including LEACH-C, Firefly Algorithm (FA), HFAPSO, FA-ANN, and HWOABCA. The GPON model reduced return loss to 25.5 dB at 3.5 GHz and improved peak gain to 4.2 dB i, while maintaining 92 % radiation efficiency. In contrast, PAN demonstrated a 15–25 % improvement in residual energy and extended network lifetime by 20 % compared to LEACH-C.

These improvements were due to the integration of advanced neural network techniques in GPON and the effective use of positional data in PAN, enabling more precise and adaptive optimization. The ability to balance multiple performance metrics simultaneously – a challenge previous models struggled with – is a key feature. This balance is crucial for UWB antennas in communication systems where both performance and energy efficiency are vital. The findings are especially relevant for practical applications in wireless sensor networks, mobile communications, and radar systems, requiring long-term network reliability and optimal antenna performance.

Keywords: ultra-wideband, antenna optimization, GPON, energy efficiency, network longevity, neural networks.

References

1. Muragesh, S. K., Rao, S. (2014). Automated internet of things for underground drainage and manhole monitoring system for metropolitan cities. International Journal of Information & Computation Technology, 4 (12), 1211–1220. Available at: https://www.ripublication.com/irph/ijict_spl/ijictv4n12spl_14.pdf
2. Haswani, N. G., Deore, P. J. (2018). Web-Based Realtime Underground Drainage or Sewage Monitoring System Using Wireless Sensor Networks. 2018 Fourth International Conference on Computing Communication Control and Automation (ICCUBEA). https://doi.org/10.1109/iccubea.2018.8697512
3. See, C. H., Kosha, J., Mshwat, W. A., Abd-Alhameed, R. A., Ong, F. L. C., McEwan, N. J., Excell, P. S. (2019). Design of mobile band subsurface antenna for drainage infrastructure monitoring. IET Microwaves, Antennas & Propagation, 13 (13), 2380–2385. https://doi.org/10.1049/iet-map.2019.0243
4. Huang, G.-L., Zhou, S.-G., Chio, T.-H. (2017). Highly-Efficient Self-Compact Monopulse Antenna System With Integrated Comparator Network for RF Industrial Applications. IEEE Transactions on Industrial Electronics, 64 (1), 674–681. https://doi.org/10.1109/tie.2016.2608769
5. Liu, G., Wang, Z., Jiang, T. (2016). QoS-Aware Throughput Maximization in Wireless Powered Underground Sensor Networks. IEEE Transactions on Communications, 64 (11), 4776–4789. https://doi.org/10.1109/tcomm.2016.2602863
6. Kunsei, H., Bialkowski, K. S., Alam, M. S., Abbosh, A. M. (2018). Improved Communications in Underground Mines Using Reconfigurable Antennas. IEEE Transactions on Antennas and Propagation, 66 (12), 7505–7510. https://doi.org/10.1109/tap.2018.2869250
7. Salam, A., Vuran, M. C., Dong, X., Argyropoulos, C., Irmak, S. (2019). A Theoretical Model of Underground Dipole Antennas for Communications in Internet of Underground Things. IEEE Transactions on Antennas and Propagation, 67 (6), 3996–4009. https://doi.org/10.1109/tap.2019.2902646
8. Shakila, R., Paramasivan, B. (2020). RETRACTED ARTICLE: An improved range based localization using Whale Optimization Algorithm in underwater wireless sensor network. Journal of Ambient In-

telligence and Humanized Computing, 12 (6), 6479–6489. https://doi.org/10.1007/s12652-020-02263-w
9. Alhawari, A. R. H., Majeed, S. F., Saeidi, T., Mumtaz, S., Alghamdi, H., Hindi, A. T. et al. (2021). Compact Elliptical UWB Antenna for Underwater Wireless Communications. Micromachines, 12 (4), 411. https://doi.org/10.3390/mi12040411
10. Mir, Z. H., Ko, Y.-B. (2020). Self-Adaptive Neighbor Discovery in Wireless Sensor Networks with Sectored-Antennas. Computer Standards & Interfaces, 70, 103427. https://doi.org/10.1016/j.csi.2020.103427
11. Ranjan, A., Sahu, H. B., Misra, P. (2020). Modeling and measurements for wireless communication networks in underground mine environments. Measurement, 149, 106980. https://doi.org/10.1016/j.measurement.2019.106980
12. Nishikawa, Y., Sasamura, T., Ishizuka, Y., Sugimoto, S., Iwasaki, S., Wang, H. et al. (2018). Design of stable wireless sensor network for slope monitoring. 2018 IEEE Topical Conference on Wireless Sensors and Sensor Networks (WiSNet). https://doi.org/10.1109/wisnet.2018.8311550
13. Salam, A., Vuran, M. C., Irmak, S. (2019). Di-Sense: In situ real-time permittivity estimation and soil moisture sensing using wireless underground communications. Computer Networks, 151, 31–41. https://doi.org/10.1016/j.comnet.2019.01.001
14. Pasupathi, S., Vimal, S., Harold-Robinson, Y., Khari, M., Verdú, E., Crespo, R. G. (2020). Energy efficiency maximization algorithm for underwater Mobile sensor networks. Earth Science Informatics, 14 (1), 215–225. https://doi.org/10.1007/s12145-020-00478-1
15. Singh, A., Mehra, R. M., Pandey, V. K. (2020). Design and Optimization of Microstrip Patch Antenna for UWB Applications Using Moth–Flame Optimization Algorithm. Wireless Personal Communications, 112 (4), 2485–2502. https://doi.org/10.1007/s11277-020-07160-1
16. Soothar, P., Wang, H., Muneer, B., Dayo, Z. A., Chowdhry, B. S. (2019). A Broadband High Gain Tapered Slot Antenna for Underwater Communication in Microwave Band. Wireless Personal Communications, 116 (2), 1025–1042. https://doi.org/10.1007/s11277-019-06633-2
17. Anveshkumar, N., Gandhi, A. S. (2017). Design and performance analysis of a modified circular planar monopole UWB antenna. 2017 8th International Conference on Computing, Communication and Networking Technologies (ICCCNT), 19, 1–5. https://doi.org/10.1109/icccnt.2017.8203970
18. Li, Y.-L., Shao, W., You, L., Wang, B.-Z. (2013). An Improved PSO Algorithm and Its Application to UWB Antenna Design. IEEE Antennas and Wireless Propagation Letters, 12, 1236–1239. https://doi.org/10.1109/lawp.2013.2283375
19. Tiemann, J., Pillmann, J., Wietfeld, C. (2017). Ultra-Wideband Antenna-Induced Error Prediction Using Deep Learning on Channel Response Data. 2017 IEEE 85th Vehicular Technology Conference (VTC Spring). https://doi.org/10.1109/vtcspring.2017.8108571
20. Yunus, F., Ariffin, S. H. S., Zahedi, Y. (2010). A Survey of Existing Medium Access Control (MAC) for Underwater Wireless Sensor Network (UWSN). 2010 Fourth Asia International Conference on Mathematical/Analytical Modelling and Computer Simulation. https://doi.org/10.1109/ams.2010.110
21. Sultan, A., Yermoldina, G., Kassym, R., Serikov, T., Bekbosynov, S., Yernazarov, N. et al. (2024). Research and construction of an adaptive drive with increased efficiency based on a balancing friction clutch. Vibroengineering Procedia, 54, 334–340. https://doi.org/10.21595/vp.2024.23971
22. Bimurzaev, S., Aldiyarov, N., Yerzhigitov, Y., Tlenshiyeva, A., Kassym, R. (2023). Improving the resolution and sensitivity of an orthogonal time-of-flight mass spectrometer with orthogonal ion injection. Eastern-European Journal of Enterprise Technologies, 6 (5 (126)), 43–54. https://doi.org/10.15587/1729-4061.2023.290649
23. Baibolov, A., Sydykov, S., Alibek, N., Tokmoldayev, A., Turdybek, B., Jurado, F., Kassym, R. (2022). Map of zoning of the territory of Kazakhstan by the average temperature of the heating period in order to select a heat pump system of heat supply: A case study. Energy Sources, Part A: Recovery, Utilization, and Environmental Effects, 44 (3), 7303–7315. https://doi.org/10.1080/15567036.2022.2108168
24. Utegenova, A., Bapyshev, A., Suimenbayeva, Z., Aden, A., Kassym, R., Tansaule, S. (2023). Development system for coordination of activities of experts in the formation of machineschetable standards in the field of military and space activities based on ontological engineering: a case study. Eastern-European Journal of Enterprise Technologies, 5 (2 (125)), 67–77. https://doi.org/10.15587/1729-4061.2023.288542

DOI: 10.15587/1729-4061.2024.309907

DEVELOPMENT MODEL OF A HIGH-PERFORMANCE MULTIPLE INPUT MULTIPLE OUTPUT MICROSTRIP ANTENNA BASED ON A PLANAR SERIES ARRAY WITH 8Ч2 ELEMENTS FOR 5G COMMUNICATION SYSTEMS (p. 37–49)

Syah Alam
Universitas Trisakti,
DKI Jakarta, Indonesia
ORCID: https://orcid.org/0000-0002-0162-8364

Indra Surjati
Universitas Trisakti,
DKI Jakarta, Indonesia
ORCID: https://orcid.org/0000-0001-6944-0213

Lydia Sari
Universitas Trisakti, DKI Jakarta, Indonesia
ORCID: https://orcid.org/0000-0003-0147-7305

Yuli Kurnia Ningsih
Universitas Trisakti,
DKI Jakarta, Indonesia
ORCID: https://orcid.org/0000-0002-1940-9143

Suryadi Suryadi
Universitas Trisakti,
DKI Jakarta, Indonesia
ORCID: https://orcid.org/0009-0006-0490-1473

Teguh Firmansyah
Universitas Sultan Ageng Tirtayasa,
Serang, Banten, Indonesia
ORCID: https://orcid.org/0000-0002-9000-9337

Zahriladha Zakaria
Universiti Teknikal Malaysia Melaka (UTeM),
Durian Tunggal, Melaka, Malaysia
ORCID: https://orcid.org/0000-0003-1467-405X

MIMO (Multiple Input Multiple Output) makes a major contribution to 5G communication systems by increasing network capacity and spectrum efficiency. In 5G, MIMO enables the use of multiple antennas at base stations and user devices, allowing simultaneous sending and receiving of data over multiple paths. This significantly increases data throughput and connection reliability, especially in environments with high user density. In addition, MIMO technology supports the implementation of beamforming, which focuses signals on a specific direction, reduces interference, and improves signal coverage and quality, making it one of the keys to achieving faster and more responsive 5G performance. Therefore, antennas with wide bandwidth, high gain and MIMO performance are crucial for supporting 5G communication systems. This paper proposes a high-performance MIMO microstrip antenna based on a series planar array with 8×2 elements operating at a resonant frequency of 3.5 GHz for 5G communication systems. A spiral stub and a feed inset are proposed to control the reflection coefficient and bandwidth of the antenna while the series planar array is proposed to increase the gain. To support the MIMO communication system, the proposed antenna is separated into two different ports with a certain distance. From the measurement results, the proposed antenna has high performance indicated by a wide bandwidth of 680 MHz (3–3.68 GHz) and a high gain of 17.8 dB at a resonant frequency of 3.5 GHz. In addition, the proposed antenna has high mutual coupling and diversity indicated by ECC and DG of 0.001 and 9.99 dB, respectively. This work provides a solution to design a high-performance microstrip antenna and can be implemented as a receiving antenna for 5G communication systems.

Keywords: microstrip antenna, high gain, MIMO system, planar array, 5G system.

References

1. Kamal, S., Bin Ain, M. F., Ullah, U., Mohammed, A. S. B., Najmi, F., Hussin, R. et al. (2021). Wheel-shaped miniature assembly of circularly polarized wideband microstrip antenna for 5G mmWave terminals. Alexandria Engineering Journal, 60 (2), 2457–2470. https://doi.org/10.1016/j.aej.2020.12.054
2. Fante, K. A., Gemeda, M. T. (2021). Broadband microstrip patch antenna at 28 GHz for 5G wireless applications. International Journal of Electrical and Computer Engineering (IJECE), 11 (3), 2238. https://doi.org/10.11591/ijece.v11i3.pp2238-2244
3. Tarpara, N., Rathwa, R. R., Kotak, D. N. A. (2018). Design of Slotted Microstrip patch Antenna for 5G Application. Int. Res. J. Eng. Technol., 5 (4), 2827–2832.
4. Hussain, R., Alreshaid, A. T., Podilchak, S. K., Sharawi, M. S. (2017). Compact 4G MIMO antenna integrated with a 5G array for current and future mobile handsets. IET Microwaves, Antennas & Propagation, 11 (2), 271–279. https://doi.org/10.1049/iet-map.2016.0738
5. Deng, J., Li, J., Zhao, L., Guo, L. (2017). A Dual-Band Inverted-F MIMO Antenna With Enhanced Isolation for WLAN Applications. IEEE Antennas and Wireless Propagation Letters, 16, 2270–2273. https://doi.org/10.1109/lawp.2017.2713986
6. Ojaroudi Parchin, N., Jahanbakhsh Basherlou, H., Al-Yasir, Y. I. A., Ullah, A., Abd-Alhameed, R. A., Noras, J. M. (2019). Multi-Band MIMO Antenna Design with User-Impact Investigation for 4G and 5G Mobile Terminals. Sensors, 19 (3), 456. https://doi.org/10.3390/s19030456
7. Hikmaturokhman, A., Ramli, K., Suryanegara, M. (2018). Spectrum Considerations for 5G in Indonesia. 2018 International Conference on ICT for Rural Development (IC-ICTRuDev). https://doi.org/10.1109/icictr.2018.8706874
8. Hobbs, S. (2018). Valuing 5G Spectrum: Valuing the 3.5 GHz and C-Band Frequency Range. Coleago Consulting.
9. An, W., Li, Y., Fu, H., Ma, J., Chen, W., Feng, B. (2018). Low-Profile and Wideband Microstrip Antenna With Stable Gain for 5G Wireless Applications. IEEE Antennas and Wireless Propagation Letters, 17 (4), 621–624. https://doi.org/10.1109/lawp.2018.2806369
10. Pratiwi, A. R., Setijadi, E., Hendrantoro, G. (2020). Design of Two-Elements Subarray with Parasitic Patch for 5G Application. 2020 International Seminar on Intelligent Technology and Its Applications (ISITIA), 7, 311–316. https://doi.org/10.1109/isitia49792.2020.9163785
11. Tang, X., Jiao, Y., Li, H., Zong, W., Yao, Z., Shan, F. et al. (2019). Ultra-Wideband Patch Antenna for Sub-6 GHz 5G Communications. 2019 International Workshop on Electromagnetics: Applications and Student Innovation Competition (IWEM). https://doi.org/10.1109/iwem.2019.8887933
12. Murugan, S. (2021). Compact MIMO Shorted Microstrip Antenna for 5G Applications. International Journal of Wireless and Microwave Technologies, 11 (1), 22–27. https://doi.org/10.5815/ijwmt.2021.01.03
13. Naik, P. S., Virani, H. G. (2020). 1×4 Microstrip Patch Slotted Array Antenna for 5G C-Band Access Point Application. 2020 International Conference on Electronics and Sustainable Communication Systems (ICESC), 1, 641–644. https://doi.org/10.1109/icesc48915.2020.9156015
14. Aghoutane, B., Das, S., EL Ghzaoui, M., Madhav, B. T. P., El Faylali, H. (2022). A novel dual band high gain 4-port millimeter wave MIMO antenna array for 28/37 GHz 5G applications. AEU - International Journal of Electronics and Communications, 145, 154071. https://doi.org/10.1016/j.aeue.2021.154071
15. Naga Jyothi Sree, G., Nelaturi, S. (2021). Design and experimental verification of fractal based MIMO antenna for lower sub 6-GHz 5G applications. AEU - International Journal of Electronics and Communications, 137, 153797. https://doi.org/10.1016/j.aeue.2021.153797
16. Hu, W., Liu, X., Gao, S., Wen, L.-H., Qian, L., Feng, T. et al. (2019). Dual-Band Ten-Element MIMO Array Based on Dual-Mode IFAs for 5G Terminal Applications. IEEE Access, 7, 178476–178485. https://doi.org/10.1109/access.2019.2958745
17. Xu, K. D., Zhu, J., Liao, S., Xue, Q. (2018). Wideband Patch Antenna Using Multiple Parasitic Patches and Its Array Application With Mutual Coupling Reduction. IEEE Access, 6, 42497–42506. https://doi.org/10.1109/access.2018.2860594
18. Alam, S., Surjati, I., Sari, L., Anindito, A., Putranto, A. Y., Firmansyah, T. (2021). Bandwidth Enhancement of Array Microstrip Antenna Using Spiral Stub For 5G Communication System. PRZEGLĄD ELEKTROTECHNICZNY, 1 (11), 42–46. https://doi.org/10.15199/48.2021.11.07
19. Alam, S., Surjati, I., Sari, L., Ningsih, Y. K., Suryadi, S., Trihantoro, G. et al. (2023). Wide band and high gain microstrip antenna using planar series array 4×2 element for 5G communication system. Eastern-European Journal of Enterprise Technologies, 4 (5 (124)), 16–24. https://doi.org/10.15587/1729-4061.2023.285395
20. Putri, S., Surjati, I., Alam, S., Ningsih, Y. K., Sari, L., Firmansyah, T., Zakaria, Z. (2024). High Isolation of Dual-Band MIMO Microstrip Antenna with Vertical – Horizontal Configuration for 5G Communication System. PRZEGLĄD ELEKTROTECHNICZNY, 1 (4), 89–95. https://doi.org/10.15199/48.2024.04.17
21. Fang, D. G. (2017). Antenna Theory and Microstrip Antennas. CRC Press. https://doi.org/10.1201/b10302
22. Garg, R., Bhartia, P., Bahl, I. J., Ittipiboon, A. (2001). Microstrip antenna design handbook. ARTECH HOUSE. Available at: https://uodiyala.edu.iq/uploads/PDF%20ELIBRARY%20UODIYALA/EL37/Microstrip%20Antenna%20Design%20Handbook.pdf

DOI: 10.15587/1729-4061.2024.313455

OPTIMIZATION OF DISTRIBUTED ACOUSTIC SENSORS BASED ON FIBER OPTIC TECHNOLOGIES (p. 50–59)

Askar Abdykadyrov
RSE "Institute of Mechanics and Engineering named after Academician U. A. Dzholdasbekova",

Almaty, Republic of Kazakhstan
Satbayev University, Almaty, Republic of Kazakhstan
ORCID: https://orcid.org/0000-0003-1143-4675

Nurzhigit Smailov
RSE "Institute of Mechanics and Engineering named after Academician U. A. Dzholdasbekova", Almaty, Republic of Kazakhstan
Satbayev University, Almaty, Republic of Kazakhstan
ORCID: https://orcid.org/0000-0002-7264-2390

Akezhan Sabibolda
RSE "Institute of Mechanics and Engineering named after Academician U. A. Dzholdasbekova", Almaty, Republic of Kazakhstan
Satbayev University, Almaty, Republic of Kazakhstan
ORCID: https://orcid.org/0000-0002-1186-7940

Gulzhaina Tolen
Satbayev University, Almaty, Republic of Kazakhstan
ORCID: https://orcid.org/0000-0002-6010-1167

Zhandos Dosbayev
RSE "Institute of Mechanics and Engineering named after Academician U. A. Dzholdasbekova", Almaty, Republic of Kazakhstan
Satbayev University, Almaty, Republic of Kazakhstan
ORCID: https://orcid.org/0000-0003-1673-4036

Zhomart Ualiyev
RSE "Institute of Mechanics and Engineering named after Academician U. A. Dzholdasbekova", Almaty, Republic of Kazakhstan
Satbayev University, Almaty, Republic of Kazakhstan
ORCID: https://orcid.org/0000-0002-5021-2154

Rashida Kadyrova
Almaty Academy of Internal Affairs of the Republic of Kazakhstan named after Makana Esbulatova, Almaty, Republic of Kazakhstan
ORCID: https://orcid.org/0009-0006-5120-6932

This research investigates distributed acoustic sensors (DAS) based on fiber optic technologies, focusing on the impact of pressure on signal-to-noise ratio (SNR), noise levels, and dominant frequency shifts. DAS systems are widely used for infrastructure monitoring due to their ability to capture acoustic signals over long distances, making them ideal for seismic and pipeline monitoring.

The study examines how fluctuating pressure affects DAS performance, particularly signal quality and noise reduction. In applications like pipeline leak detection and seismic monitoring, pressure changes can degrade signal clarity and complicate anomaly detection. Understanding this relationship is key to optimizing DAS performance and improving system efficiency.

The experiment varied pressure from 0.1 atm to 5 atm, showing that increased pressure raised SNR from 10 dB to 48 dB, reduced noise from 10 dB to 7 dB, and shifted the dominant frequency from 0.5 Hz to 3 Hz. Fourier analysis provided insights into these frequency spectrum changes. Higher pressure compresses the medium, enhancing signal isolation and improving SNR while reducing noise. The frequency shift results from changes in acoustic wave propagation speed under higher pressure, highlighting its role in signal processing.

The key finding is that higher pressure significantly improves signal quality and reduces noise, enhancing DAS performance. The frequency shift improves environmental detection capabilities. These results are valuable for DAS applications in environments with pressure variations, like pipeline monitoring, where high signal quality is crucial. Improved signal fidelity and frequency shifts make DAS systems more reliable for long-term monitoring and contribute to accurate anomaly detection.

Keywords: fiber optic technologies, distributed acoustic sensors, seismic monitoring, infrastructure monitoring.

References

1. Udd, E., Spillman, W. B. (Eds.) (2024). Fiber Optic Sensors. John Wiley & Sons, Inc. https://doi.org/10.1002/9781119678892
2. Ashry, I., Mao, Y., Wang, B., Hveding, F., Bukhamsin, A., Ng, T. K., Ooi, B. S. (2022). A Review of Distributed Fiber–Optic Sensing in the Oil and Gas Industry. Journal of Lightwave Technology, 40 (5), 1407–1431. https://doi.org/10.1109/jlt.2021.3135653
3. Hveding, F., Bukhamsin, A. (2018). Distributed Fiber Optic Sensing – A Technology Review for Upstream Oil and Gas Applications. All Days. https://doi.org/10.2118/192323-ms
4. Mikhailov, P., Ualiyev, Z., Kabdoldina, A., Smailov, N., Khikmetov, A., Malikova, F. (2021). Multifunctional fiber-optic sensors for space infrastructure. Eastern-European Journal of Enterprise Technologies, 5 (5 (113)), 80–89. https://doi.org/10.15587/1729-4061.2021.242995
5. Sekenov, B., Smailov, N., Tashtay, Y., Amir, A., Kuttybayeva, A., Tolemanova, A. (2024). Fiber-Optic Temperature Sensors for Monitoring the Influence of the Space Environment on Nanosatellites: A Review. Advances in Asian Mechanism and Machine Science, 371–380. https://doi.org/10.1007/978-3-031-67569-0_42
6. Khabay, A., Baktybayev, M., Ibekeyev, S., Sarsenbayev, N., Junussov, N., Zhumakhan, N. (2024). Improvement of fiber optic sensor measurement methods for temperature and humidity measurement in microelectronic circuits. Eastern-European Journal of Enterprise Technologies, 3 (5 (129)), 36–44. https://doi.org/10.15587/1729-4061.2024.306711
7. Parker, T., Shatalin, S., Farhadiroushan, M. (2014). Distributed Acoustic Sensing – a new tool for seismic applications. First Break, 32 (2). https://doi.org/10.3997/1365-2397.2013034
8. Masoudi, A., Newson, T. P. (2016). Contributed Review: Distributed optical fibre dynamic strain sensing. Review of Scientific Instruments, 87 (1). https://doi.org/10.1063/1.4939482
9. Hartog, A. H. (2017). An Introduction to Distributed Optical Fibre Sensors. CRC Press. https://doi.org/10.1201/9781315119014
10. Gonzalez-Herraez, M., Fernandez-Ruiz, M. R., Magalhaes, R., Costa, L., Martins, H. F., Becerril, C. et al. (2021). Distributed Acoustic Sensing for Seismic Monitoring. Optical Fiber Communication Conference (OFC) 2021, 9, Tu1L.2. https://doi.org/10.1364/ofc.2021.tu1l.2
11. Dou, S., Lindsey, N., Wagner, A. M., Daley, T. M., Freifeld, B., Robertson, M. et al. (2017). Distributed Acoustic Sensing for Seismic Monitoring of The Near Surface: A Traffic-Noise Interferometry Case Study. Scientific Reports, 7 (1). https://doi.org/10.1038/s41598-017-11986-4
12. Zhu, H.-H., Liu, W., Wang, T., Su, J.-W., Shi, B. (2022). Distributed Acoustic Sensing for Monitoring Linear Infrastructures: Current Status and Trends. Sensors, 22 (19), 7550. https://doi.org/10.3390/s22197550
13. Martins, W. A., de Campos, M. L. R., da Silva Chaves, R., Lordelo, C. P. V., Ellmauthaler, A., Nunes, L. O., Barfoot, D. A. (2017). Communication Models for Distributed Acoustic Sensing for Telemetry. IEEE Sensors Journal, 17 (15), 4677–4688. https://doi.org/10.1109/jsen.2017.2714023
14. Wang, Y., Yuan, H., Liu, X., Bai, Q., Zhang, H., Gao, Y., Jin, B. (2019). A Comprehensive Study of Optical Fiber Acoustic Sensing. IEEE Access, 7, 85821–85837. https://doi.org/10.1109/access.2019.2924736

15. Cannon, R., Aminzadeh, F. (2013). Distributed Acoustic Sensing: State of the Art. All Days. https://doi.org/10.2118/163688-ms
16. Soroush, M., Mohammadtabar, M., Roostaei, M., Hosseini, S. A., Fattahpour, V., Mahmoudi, M. et al. (2022). Downhole Monitoring Using Distributed Acoustic Sensing: Fundamentals and Two Decades Deployment in Oil and Gas Industries. Day 3 Wed, March 23, 2022. https://doi.org/10.2118/200088-ms
17. Johannessen, K., Drakeley, B., Farhadiroushan, M. (2012). Distributed Acoustic Sensing - A New Way of Listening to Your Well/Reservoir. All Days. https://doi.org/10.2118/149602-ms
18. Lindsey, N. J., Martin, E. R., Dreger, D. S., Freifeld, B., Cole, S., James, S. R. et al. (2017). Fiber Optic Network Observations of Earthquake Wavefields. Geophysical Research Letters, 44 (23). https://doi.org/10.1002/2017gl075722
19. Zhan, Z. (2019). Distributed Acoustic Sensing Turns Fiber-Optic Cables into Sensitive Seismic Antennas. Seismological Research Letters, 91 (1), 1–15. https://doi.org/10.1785/0220190112
20. Sladen, A., Rivet, D., Ampuero, J. P., De Barros, L., Hello, Y., Calbris, G., Lamare, P. (2019). Distributed sensing of earthquakes and ocean-solid Earth interactions on seafloor telecom cables. Nature Communications, 10 (1). https://doi.org/10.1038/s41467-019-13793-z
21. Murayama, H., Wada, D., Igawa, H. (2013). Structural health monitoring by using fiber-optic distributed strain sensors with high spatial resolution. Photonic Sensors, 3 (4), 355–376. https://doi.org/10.1007/s13320-013-0140-5
22. Eum, S. H., Kageyama, K., Murayama, H., Uzawa, K., Ohsawa, I., Kanai, M. et al. (2007). Structural health monitoring using fiber optic distributed sensors for vacuum-assisted resin transfer molding. Smart Materials and Structures, 16 (6), 2627–2635. https://doi.org/10.1088/0964-1726/16/6/067
23. Fan, X., He, Z., Liu, Q., Chen, D., Wang, S., Yang, G. (2018). Fiber-optic distributed acoustic sensors (DAS) and applications in railway perimeter security. Advanced Sensor Systems and Applications VIII, 28, 1. https://doi.org/10.1117/12.2505342
24. Ružička, M., Münster, P., Dejdar, P., Jablončík, L. (2021). Distributed optical fiber acoustic sensing system for perimeter security. Security & Future, 5 (4), 150–152. Available at: https://stumejournals.com/journals/confsec/2021/4/150.full.pdf
25. Kabdoldina, A., Ualiyev, Z., Smailov, N., Malikova, F., Oralkanova, K., Baktybayev, M. et al. (2022). Development of the design and technology for manufacturing a combined fiber-optic sensor used for extreme operating conditions. Eastern-European Journal of Enterprise Technologies, 5 (5 (119)), 34–43. https://doi.org/10.15587/1729-4061.2022.266359
26. Smailov, N., Zhadiger, T., Tashtay, Y., Abdykadyrov, A., Amir, A. (2024). Fiber laser-based two-wavelength sensors for detecting temperature and strain on concrete structures. International Journal of Innovative Research and Scientific Studies, 7 (4), 1693–1710. https://doi.org/10.53894/ijirss.v7i4.3481
27. Kuttybayeva, A., Sabibolda, A., Kengesbayeva, S., Baigulbayeva, M., Amir, A., Sekenov, B. (2024). Investigation of a Fiber Optic Laser Sensor with Grating Resonator Using Mirrors. 2024 Conference of Young Researchers in Electrical and Electronic Engineering (ElCon). https://doi.org/10.1109/elcon61730.2024.10468264
28. Sabibolda, A., Tsyporenko, V., Smailov, N., Tsyporenko, V., Abdykadyrov, A. (2024). Estimation of the Time Efficiency of a Radio Direction Finder Operating on the Basis of a Searchless Spectral Method of Dispersion-Correlation Radio Direction Finding. Advances in Asian Mechanism and Machine Science, 62–70. https://doi.org/10.1007/978-3-031-67569-0_8
29. Smailov, N., Tsyporenko, V., Sabibolda, A., Tsyporenko, V., Kabdoldina, A., Zhekambayeva, M. et al. (2023). Improving the accuracy of a digital spectral correlation-interferometric method of direction finding with analytical signal reconstruction for processing an incomplete spectrum of the signal. Eastern-European Journal of Enterprise Technologies, 5 (9 (125)), 14–25. https://doi.org/10.15587/1729-4061.2023.288397
30. Sabibolda, A., Tsyporenko, V., Tsyporenko, V., Smailov, N., Zhunussov, K., Abdykadyrov, A. et al. (2022). Improving the accuracy and performance speed of the digital spectral-correlation method for measuring delay in radio signals and direction finding. Eastern-European Journal of Enterprise Technologies, 1 (9(115)), 6–14. https://doi.org/10.15587/1729-4061.2022.252561

DOI: **10.15587/1729-4061.2024.312489**

IDENTIFICATION OF CHARACTERISTICS OF CONCEPTUAL PROTOTYPE OF MICROPROCESSOR RESOURCE-SAVING RELAY PROTECTION SYSTEM (p. 60–69)

Alexandr Neftissov
Astana IT University, Astana, Republic of Kazakhstan
ORCID: https://orcid.org/0000-0003-4079-2025

Ilyas Kazambayev
Astana IT University, Astana, Republic of Kazakhstan
ORCID: https://orcid.org/0000-0003-0850-7490

Lalita Kirichenko
Astana IT University, Astana, Republic of Kazakhstan
ORCID: https://orcid.org/0000-0001-7069-5395

Dnislam Urazayev
Nazarbayev University, Astana, Republic of Kazakhstan
ORCID: https://orcid.org/0000-0002-4542-2691

Andrii Biloshchytskyi
Astana IT University, Astana, Republic of Kazakhstan
Kyiv National University of Construction and Architecture, Kyiv, Ukraine
ORCID: https://orcid.org/0000-0001-9548-1959

Omirzak Abdirashev
L. N. Gumilyov Eurasian National University, Astana, Republic of Kazakhstan
ORCID: https://orcid.org/0000-0001-7621-5444

The object of the study is the conceptual prototype of a microprocessor resource-saving relay protection system. Currently, relay protection ensures electrical networks reliable and efficient work, however, the traditional architecture is proprietary, not allowing to fix and replace damaged parts without a company specialist. Therefore, the open-architecture relay protection is a very pressing issue, but the problem lies in meeting the relay protection requirements. The data transmission protocols nRF and ESP-NOW, Hall sensors evaluation for AC current measurement determination and sensor accuracy improvement was implemented. Experimental validation demonstrated that nRF and ESP-NOW protocols meet the delay and reliability requirements, however, the nRF protocol is more suitable due to its flexibility and obstacle penetration. The data demonstrated that the most effective conditions are without obstacles at 15 meters from the modem and with obstacles 5 meters from the modem. The experiment of Hall sensors characteristics determination

demonstrated the accuracy of current measurement with the set values of the opening and closing currents. Nevertheless, it is not accurate (12.45 %) for the relay protection application. Therefore, the application of the changing values of the opening and closing currents is more effective and accuracy reaches 6.92 %. As a result, the service life of the Hall sensor was determined, and even after 10 million openings, the open state time remained unchanged. Therefore, the approximation function for current amplitude determination depending on open state time was found. On the other hand, Hall sensors may suffer from temperature drift and require further optimization to be fully reliable. The study limitation is the current range from 0 to 800 A.

Keywords: relay protection, reed switch, Hall sensor, magnetic field, open architecture.

References

1. Technical report on the events of 9 august 2019. Available at: https://www.ofgem.gov.uk/sites/default/files/docs/2019/09/eso_technical_report_-_final.pdf
2. Bringing 5G to power. Available at: https://www.ericsson.com/en/reports-and-papers/industrylab/reports/bringing-5g-to-power
3. Biglarbegian, M., Nibir, S. J., Jafarian, H., Parkhideh, B. (2016). Development of current measurement techniques for high frequency power converters. 2016 IEEE International Telecommunications Energy Conference (INTELEC). https://doi.org/10.1109/intlec.2016.7749133
4. Shen, D., Hu, B., Wang, X., Zhu, M., Wang, L., Lu, W. (2017). Research on Harmonic Characteristic of Electronic Current Transformer Based on the Rogowski Coil. IOP Conference Series: Materials Science and Engineering, 199, 012123. https://doi.org/10.1088/1757-899x/199/1/012123
5. Piesciorovsky, E. C., Warmack, R. J. B., Polsky, Y. (2023). Medium-Voltage Testbed for Comparing Advanced Power Line Sensors vs. Measurement Transformers with Electrical Grid Events. Energies, 16 (13), 4944. https://doi.org/10.3390/en16134944
6. Chen, J., Xu, Q., Wang, K. (2020). Research and Application of Generator Protection Based on Fiber Optical Current Transformer. IEEE Access, 8, 172405–172411. https://doi.org/10.1109/access.2020.3018734
7. Parkhomenko, R., Aniskov, O., Tsibulevsky, Y., Melnik, O., Shchokina, O., Kharitonov, A. et al. (2018). Designing a combined device for determining the place of arc discharge. Eastern-European Journal of Enterprise Technologies, 3 (5 (93)), 12–18. https://doi.org/10.15587/1729-4061.2018.134016
8. Kletsel, M. Ya., Mashrapov, B. E., Mashrapova, R. M. (2023). Reed switch protection of double-circuit lines without current and voltage transformers. International Journal of Electrical Power & Energy Systems, 154, 109457. https://doi.org/10.1016/j.ijepes.2023.109457
9. Kletsel, M., Mashrapov, B., Mashrapova, R. (2024). Resource-saving microprocessor-based reed switch current protection. Electric Power Systems Research, 230, 110276. https://doi.org/10.1016/j.epsr.2024.110276
10. Goryunov, V., Kletsel, M., Mashrapov, B., Mussayev, Z., Talipov, O. (2022). Resource-saving current protections for electrical installations with isolated phase busducts. Alexandria Engineering Journal, 61 (8), 6061–6069. https://doi.org/10.1016/j.aej.2021.11.031
11. Issabekov, D. D., Mussayev, Z. B., Markovskiy, V. P., Kislov, A. P., Urazalimova, D. S. (2024). Reed Switch Overcurrent Protection: New Approach to Design. Energies, 17 (11), 2481. https://doi.org/10.3390/en17112481
12. Blagojević, M., Jovanović, U., Jovanović, I., Mančić, D. (2017). Folded bus bar current transducer based on Hall effect sensor. Electrical Engineering, 100 (2), 1243–1251. https://doi.org/10.1007/s00202-017-0579-2
13. Weiss, R., Itzke, A., ReitenspieB, J., Hoffmann, I., Weigel, R. (2019). A Novel Closed Loop Current Sensor Based on a Circular Array of Magnetic Field Sensors. IEEE Sensors Journal, 19 (7), 2517–2524. https://doi.org/10.1109/jsen.2018.2887302
14. Xu, Y., Lalwani, A. V., Arora, K., Zheng, Z., Renteria, A., Senesky, D. G., Wang, P. (2022). Hall-Effect Sensor Design With Physics-Informed Gaussian Process Modeling. IEEE Sensors Journal, 22 (23), 22519–22528. https://doi.org/10.1109/jsen.2022.3216499
15. Neftissov, A., Sarinova, A., Kazambayev, I., Kirichenko, L., Kuchanskyi, O., Faizullin, A. (2023). Determination of the speed of a microprocessor relay protection device of open architecture with a reed switch and the industrial internet of things. Eastern-European Journal of Enterprise Technologies, 2 (5 (122)), 20–30. https://doi.org/10.15587/1729-4061.2023.276588
16. Neftissov, A., Sarinova, A., Kazambayev, I., Kirichenko, L., Biloshchytskyi, A., Kislov, A., Andreyeva, O. (2023). Development of the error reducing method for the determination of the alternating current amplitude without the use of current transformers. Eastern-European Journal of Enterprise Technologies, 5 (5 (125)), 32–42. https://doi.org/10.15587/1729-4061.2023.288339

DOI: 10.15587/1729-4061.2024.313747

DEVELOPMENT OF MATHEMATICAL MODELS OF HEAT CONDUCTIVITY FOR MODERN ELECTRONIC DEVICES WITH ELEMENTS CONTAINING FOREIGN INCLUSIONS (p. 70–79)

Vasyl Havrysh
Lviv Polytechnic National University,
Lviv, Ukraine
ORCID: https://orcid.org/0000-0003-3092-2279

Elvira Dzhumelia
Lviv Polytechnic National University,
Lviv, Ukraine
ORCID: https://orcid.org/0000-0003-3146-8725

Oksana Hrytsai
Lviv Polytechnic National University,
Lviv, Ukraine
ORCID: https://orcid.org/0000-0003-0710-1675

Stepan Kachan
Lviv Polytechnic National University,
Lviv, Ukraine
ORCID: https://orcid.org/0000-0003-0306-9110

Viktoria Maikher
Lviv Polytechnic National University,
Lviv, Ukraine
ORCID: https://orcid.org/0000-0003-0786-6950

This paper considers the heat conduction process for an isotropic medium containing a foreign half-through inclusion and heated by a locally concentrated heat flow. Linear and non-linear mathematical models for determining the temperature field have been built to establish the temperature regimes for the effective operation of electronic devices. The coefficient of thermal conductivity of a non-uniform structure is represented as a whole, using asymmetric unit functions, which automatically provides the conditions of ideal thermal contact on the surfaces of materials. This results in solving one heat conduction equation with discontinuous and singular coefficients. A linearizing function was introduced to linearize the nonlinear boundary value problem. Analytical-numerical solutions

of linear and nonlinear boundary-value problems have been obtained in a closed form. A linear temperature dependence of the coefficient of thermal conductivity of structural materials was chosen for a heat-sensitive medium. As a result, an analytical-numerical solution was derived, which determines the temperature distribution in this medium. On this basis, a numerical experiment was performed, the results of which are graphically displayed and confirm the adequacy of the constructed mathematical models to a real physical process.

The materials of the plate and inclusion are silicon and silver. The results for these materials based on the linear and non-linear model differ by 7 %. Their slight difference is explained by the fact that the values of the temperature coefficient of thermal conductivity are small. The models built make it possible to analyze the given environments in terms of their thermal resistance. As a result, it becomes possible to improve it, and protect structures from overheating, which could lead to the failure of individual nodes and their elements and the entire electronic device.

Keywords: thermal resistance of the structure, foreign half-through inclusion, ideal thermal contact, convective heat exchange.

References

1. Sheikh, Z. (1994). Where do you the cooling vents. Electronics cooling.
2. Zhang, Z., Sun, Y., Cao, X., Xu, J., Yao, L. (2024). A slice model for thermoelastic analysis of porous functionally graded material sandwich beams with temperature-dependent material properties. Thin-Walled Structures, 198, 111700. https://doi.org/10.1016/j.tws.2024.111700
3. Zhang, Z., Zhou, D., Fang, H., Zhang, J., Li, X. (2021). Analysis of layered rectangular plates under thermo-mechanical loads considering temperature-dependent material properties. Applied Mathematical Modelling, 92, 244–260. https://doi.org/10.1016/j.apm.2020.10.036
4. Peng, X., Li, X., Gong, Z., Zhao, X., Yao, W. (2022). A deep learning method based on partition modeling for reconstructing temperature field. International Journal of Thermal Sciences, 182, 107802. https://doi.org/10.1016/j.ijthermalsci.2022.107802
5. Ren, Y., Huo, R., Zhou, D., Zhang, Z. (2022). Thermo-Mechanical Buckling Analysis of Restrained Columns Under Longitudinal Steady-State Heat Conduction. Iranian Journal of Science and Technology, Transactions of Civil Engineering, 47 (3), 1411–1423. https://doi.org/10.1007/s40996-022-01020-7
6. Breukelman, H. J., Santofimia, M. J., Hidalgo, J. (2023). Dataset of a thermal model for the prediction of temperature fields during the creation of austenite/martensite mesostructured materials by localized laser treatments in a Fe-Ni-C alloy. Data in Brief, 48, 109110. https://doi.org/10.1016/j.dib.2023.109110
7. Zhang, W., Wu, M., Du, S., Chen, L., Hu, J., Lai, X. (2023). Modeling of Steel Plate Temperature Field for Plate Shape Control in Roller Quenching Process. IFAC-PapersOnLine, 56 (2), 6894–6899. https://doi.org/10.1016/j.ifacol.2023.10.493
8. Khan, Z. H., Khan, W. A., Ibrahim, S. M., Mabood, F., Huang, Z. (2024). Effects of thermal boundary conditions on Stokes' second problem. Results in Physics, 60, 107662. https://doi.org/10.1016/j.rinp.2024.107662
9. Evstatieva, N., Evstatiev, B. (2023). Modelling the Temperature Field of Electronic Devices with the Use of Infrared Thermography. 2023 13th International Symposium on Advanced Topics in Electrical Engineering (ATEE), 1–5. https://doi.org/10.1109/atee58038.2023.10108375
10. Liu, H., Yu, J., Wang, R. (2023). Dynamic compact thermal models for skin temperature prediction of portable electronic devices based on convolution and fitting methods. International Journal of Heat and Mass Transfer, 210, 124170. https://doi.org/10.1016/j.ijheatmasstransfer.2023.124170
11. Ghannad, M., Yaghoobi, M. P. (2015). A thermoelasticity solution for thick cylinders subjected to thermo-mechanical loads under various boundary conditions. International Journal of Advanced Design & Manufacturing Technology, 8 (4).
12. Song, H., Song, K., Gao, C. (2019). Temperature and thermal stress around an elliptic functional defect in a thermoelectric material. Mechanics of Materials, 130, 58–64. https://doi.org/10.1016/j.mechmat.2019.01.008
13. Parhizkar Yaghoobi, M., Ghannad, M. (2020). An analytical solution for heat conduction of FGM cylinders with varying thickness subjected to non-uniform heat flux using a first-order temperature theory and perturbation technique. International Communications in Heat and Mass Transfer, 116, 104684. https://doi.org/10.1016/j.icheatmasstransfer.2020.104684
14. Eker, M., Yarımpabuç, D., Çelebi, K. (2020). Thermal stress analysis of functionally graded solid and hollow thick-walled structures with heat generation. Engineering Computations, 38 (1), 371–391. https://doi.org/10.1108/ec-02-2020-0120
15. Wang, H., Qin, Q. (2019). Thermal Analysis of a Functionally Graded Coating/Substrate System Using the Approximated Transfer Approach. Coatings, 9 (1), 51. https://doi.org/10.3390/coatings9010051
16. Zhang, Q., Song, H., Gao, C. (2023). The 3-D problem of temperature and thermal flux distribution around defects with temperature-dependent material properties. Thermal Science, 27 (5 Part B), 3903–3920. https://doi.org/10.2298/tsci221003028z
17. Havrysh, V. I., Kolyasa, L. I., Ukhanska, O. M., Loik, V. B. (2019). Determination of temperature field in thermally sensitive layered medium with inclusions. Naukovyi Visnyk Natsionalnoho Hirnychoho Universytetu, 1, 76–82. https://doi.org/10.29202/nvngu/2019-1/5
18. Havrysh, V. I. (2017). Investigation of Temperature Fields in a Heat-Sensitive Layer with Through Inclusion. Materials Science, 52 (4), 514–521. https://doi.org/10.1007/s11003-017-9984-y
19. Havrysh, V. I., Kosach, A. I. (2012). Boundary-value problem of heat conduction for a piecewise homogeneous layer with foreign inclusion. Materials Science, 47 (6), 773–782. https://doi.org/10.1007/s11003-012-9455-4
20. Gavrysh, V., Tushnytskyy, R., Pelekh, Y., Pukach, P., Baranetskyi, Y. (2017). Mathematical model of thermal conductivity for piecewise homogeneous elements of electronic systems. 2017 14th International Conference The Experience of Designing and Application of CAD Systems in Microelectronics (CADSM), 50, 333–336. https://doi.org/10.1109/cadsm.2017.7916146

DOI: 10.15587/1729-4061.2024.314117

DEVISING A METHOD FOR DETERMINING THE MOISTURE CONDUCTIVITY COEFFICIENT OF SUBGRADE SOILS TAKING INTO ACCOUNT EUROPEAN APPROACHES AND STANDARDS (p. 80–89)

Andrii Bubela
National Transport University, Kyiv, Ukraine
ORCID: http://orcid.org/0000-0002-5619-003X

Liudmyla Bondarenko
National Transport University, Kyiv, Ukraine
ORCID: http://orcid.org/0000-0002-8239-065X

Yevheniia Kvatadze
National Transport University, Kyiv, Ukraine
ORCID: https://orcid.org/0000-0003-2798-8955

Andrii Ivko
Kyiv National University of Construction and Architecture, Kyiv, Ukraine
ORCID: https://orcid.org/0000-0002-3388-8355

Vitalii Stozhka
National Transport University, Kyiv, Ukraine
ORCID: https://orcid.org/0000-0002-5039-9852

The object of this study is the theoretical and methodological approaches to determining the coefficient of moisture conductivity of subgrade soils. The work focuses on considering the European approaches and standards when devising a method for determining the coefficient of moisture conductivity of soils.

In the course of the research, a method was developed for determining the coefficient of moisture conductivity of soils K_1, which characterizes the diffusion movement of water, through the filtration coefficient K_0, calculated in accordance with European requirements based on laboratory test data.

The proposed method is based on a mathematical model built on the basis of the differential equation of changes in soil moisture. The model is special in that, unlike existing ones, the movement of water was modeled from the bottom up, which reflects the process of moisture accumulation in the lower layers of the subgrade from groundwater or topwater.

A good agreement of the mathematical model with the data by other authors was obtained (the relative error did not exceed 12.98 %).

A direct relationship between the moisture conductivity coefficient of soils K_1 and their initial moisture content W_0 and an inverse relationship between K_1 and the total moisture capacity of soils W_{FH} were established in the paper. Dependences were derived in the range of changes in initial soil moisture W_0 from 0.08 to 0.15 and W_{FH} from 0.15 to 0.5. It was found that the values of the moisture conductivity coefficient of soils K_1 increase from $4.64 \cdot 10^{-6}$ to $3.81 \cdot 10^{-5}$ m^2/h with an increase in their initial moisture content and with a decrease in total moisture capacity.

From the point of view of engineering practice of road construction, the proposed method makes it possible to predict seasonal changes in soil moisture in the subgrade, to determine the strength of the road structure. This makes it possible to make sound design decisions on the installation of drainage systems on roads in order to extend their service life.

Keywords: soil moisture, coefficient of soil moisture conductivity, subgrade, road structure.

References

1. Sawangsuriya, A., Wachiraporn, S., Sramoon, W. (2015). Soil moisture and strength index for earthwork construction quality control. IOP Conference Series: Earth and Environmental Science, 26, 012033. https://doi.org/10.1088/1755-1315/26/1/012033
2. Getachew, D. (2022) Determination of Effect of Moisture Content and Density on Shear Strength Parameters and Slope Stability of Highly Plastic Silt Embankment Soil (the Case of Wozeka-Gidole Road). International research journal of engineering and technology, 7, 2333–2346. Available at: https://www.researchgate.net/publication/359218718_INTERNATIONAL_RESEARCH_JOURNAL_OF_ENGINEERING_AND_TECHNOLOGY_IRJET_Determination_of_Effect_of_Moisture_Content_and_Density_on_Shear_Strength_Parameters_and_Slope_Stability_of_Highly_Plastic_Silt_Emban
3. Nguyen, T. M., Walker, J. P., Ye, N., Kodikara, J. (2023). Use of an L-band radiometer for proximal moisture measurement in road construction. Transportation Geotechnics, 38, 100876. https://doi.org/10.1016/j.trgeo.2022.100876
4. Venmans, A. A. M., van de Ven, R., Kollen, J. (2016). Rapid and Non-intrusive Measurements of Moisture in Road Constructions Using Passive Microwave Radiometry and GPR – Full Scale Test. Procedia Engineering, 143, 1244–1251. https://doi.org/10.1016/j.proeng.2016.06.111
5. Shan, W., Guo, Y. (2009). The effect of plant root system on temperature and moisture of road cutting slope in seasonal frozen regions. Geophysical Research Abstracts, 11. Available at: https://www.researchgate.net/publication/234452799_The_effect_of_plant_root_system_on_temperature_and_moisture_of_road_cutting_slope_in_seasonal_frozen_regions
6. Uduebor, M., (2023) Engineered water repellency for moisture control in pavement soils. Graduate Research Symposium. Charlotte. Available at: https://www.researchgate.net/publication/372162478_ENGINEERED_WATER_REPELLENCY_FOR_MOISTURE_CONTROL_IN_PAVEMENT_SOILS
7. Bondarenko, L., Kvatadze, Y. (2022). Methods of determining the coefficient of moisture conductivity of soils subgrade. Dorogi i Mosti, 2022 (26), 138–146. https://doi.org/10.36100/dorogimosti2022.26.138
8. ISO 17892-11:2019 (E) Geotechnical investigation and testing – Laboratory testing of soil – Part 11: Permeability tests. Available at: https://www.iso.org/ru/standard/72016.html
9. M 42.1-37641918-785:2023 Metodyka vyznachennia koefitsiienta volohoprovidnosti gruntiv zemlianoho polotna na avtomobilnykh dorohakh zahalnoho korystuvannia (2023). Kyiv, 33. Available at: https://online.budstandart.com/ua/catalog/doc-page.html?id_doc=106753
10. Puzakov, N. A., Zolotar, Y. A., Sydenko, V. M., Tulaev, A. Ya. et al. (1971). Vodno-teplovoi rezhym zemlianoho polotna y dorozhnikh odezhd. Moscow: Transport, 413.

DOI: 10.15587/1729-4061.2024.313114

DETERMINING WORKING CHARACTERISTICS OF THE EXCESS AIR PRESSURE SYSTEM IN AN EMERGENCY HATCH BASED ON JET WATER-GAS EJECTORS (p. 90–99)

Serhii Hrynchak
Naval Institute of the National University "Odesa Maritime Academy", Odesa, Ukraine
ORCID: https://orcid.org/0000-0001-6627-7780

The object of this study is jet water and gas ejectors in the fire safety system of ships. The problem solved relates to the fact that in the event of a fire in the area of the exit from the ship's emergency room, the heat energy increases dangerously and a large amount of smoke spreads throughout the ship's rooms. These factors require immediate sealing of the emergency room, which limits the immediate access of emergency teams to the room. Installation of a local excess air pressure system in the emergency hatch on the basis of jet water and gas ejectors could make it possible to shield thermal energy and localize smoke gases in the emergency room without sealing it to ensure prompt access of emergency teams to it. The following results were achieved – the adequacy of theoretical studies of the processes of localization of flue gases in the emergency room without its sealing was confirmed by the experimental method. The investigated problem was solved by optimizing processes: the rate of change in the natural indicator of the weakening of environment during the start-up of the local excess air pressure system in the emergency hatch based on jet water and gas ejectors; the effectiveness of reducing the temperature of heated gases in the superstructure during the operation of the excess air pressure system in the emergency hatch based on jet water-gas ejectors. Special feature of the results was the formation of an air curtain obtained by the selection of a part of high-temperature flue gases in the housings of jet water-gas ejectors, their heat-mass exchange processing and output back into the flow. This created conditions under which thermal energy is shielded with an efficiency of 85–88 %. The scope and conditions of practical use of the results are shipbuilding and ship fire safety design.

Keywords: water-gas jet ejector, emergency hatch, natural attenuation index, thermal energy.

References

1. Hrynchak, S. (2024). Determining performance characteristics of jet water-gas ejectors for an opening in a vertical fencing structure. Eastern-European Journal of Enterprise Technologies, 3 (10 (129)), 21–32. https://doi.org/10.15587/1729-4061.2024.305828
2. Miroshnichenko, V. N., Sokolov, V. V., Sheverev, E. Iu. et al. (2002). Issledovanie dymoosazhdaiushchei i okhlazhdaiushchei effektivnosti ustroistv UDP GIBK. 065289.001. Naukovii visnik UkrNDIPB, 1 (5), 76–82.
3. Zatcarinnaia, T. G. (2004). Lokalizatciia gazovozdushnogo potoka (dyma) vodianoi zavesoi reguliruemoi tolshchiny orosheniia. Zbirnik naukovikh pratc, 1 (4), 238–243.
4. Kuripko, O. V., Nikitin, E. V., Anokhin, G. A. (2002). Povyshenie ognestoikosti korabelnykh ograzhdaiushchikh konstruktcii: puti i metody issledovanii. Zbirnik naukovikh pratc, 1, 164–169.
5. Blintsov, V., Hrynchak, S. (2017). Development of the improved methods of fight against distribution of smoke on ship with systems of jet water–gas ejectors. EUREKA: Physics and Engineering, 6, 35–41. https://doi.org/10.21303/2461-4262.2017.00498
6. Blintsov, V. S., Hrynchak, S. O. (2017). Theoretical substantiation of the method for designing ship apertures with the use of the air suppression system based on the jet water-gas apparatus. Collection of Scientific Publications NUS, 470 (3), 11–20. https://doi.org/10.15589/jnn20170302
7. Hrynchak, S. O. (2016). Pat. No. 110777 UA. Sposib pidporu povitria v avariinomu liuku i prystrii dlia yoho realizatsii. MPK A62C 3/00. No. a201206290; declareted: 24.05.2012; published: 25.02.2016, Bul. No. 4, 4.
8. Mayerhöfer, T. G., Pahlow, S., Popp, J. (2020). The Bouguer-Beer-Lambert Law: Shining Light on the Obscure. ChemPhysChem, 21 (18), 2029–2046. https://doi.org/10.1002/cphc.202000464
9. Oehlert, G. W. (2010). A first course in design and analysis of experiments. Minneapolis: University of Minnesota Press, 679.
10. Jiju, A. (2014). Design of Experiments for Engineers and Scientists. Elsevier Ltd, 276. https://doi.org/10.1016/c2012-0-03558-2
11. Design of Engineering Experiments. Available at: https://www.studysmarter.co.uk/explanations/engineering/professional-engineering/design-of-engineering-experiments/ Last accessed: 08.04.2024
12. Roy, R. K. (2001). Design of experiments using the taguchi approach: 16 Steps to product and process improvement. John Wiley & Sons, Inc., 544.

АНОТАЦІЇ

APPLIED MECHANICS

DOI: 10.15587/1729-4061.2024.314234

ОПТИМІЗАЦІЯ СОНЯЧНОГО ЕЛЕМЕНТА НА ОСНОВІ ТЕЛУРИДУ КАДМІЮ ШЛЯХОМ ВНЕСЕННЯ ПОГЛИНАЮЧОГО ШАРУ CdSeTe (МОДЕЛЮВАННЯ ГЕТЕРОСТРУКТУРИ) (с. 6–12)

Г. А. Ільчук, І. В.Семків, М. С. Каркульовська, В. М. Ващинський, М. В. Соловйов

Сонячні елементи на основі телуриду кадмію є одними із найпоширеніших пристроїв для фотоелектричних застосувань. Однак ефективність перетворення енергії цих елементів залишається недостатньо високою. Використовуючи програмне середовище SCAPS проведено дослідження та оптимізацію класичного тонкоплівкового сонячного елемента на основі CdTe. Структура цього елемента складалася з ITO в якості прозорого провідного контакту, шару сульфіду кадмію (CdS) і шару поглинача телуриду кадмію (CdTe) з металевим контактом. Для оптимізації такої конструкції з точки зору ефективності перетворення потужності, розглянуто вплив товщини та концентрації домішок акцепторів в поглинаючому шарі CdTe, а також вплив товщини та концентрації домішок донорів в буферному CdS шарі. Встановлено, що отимальні товщини для буферного шару CdS та поглинаючого CdTe шарів відповідно становлять 50 нм та 3000 нм. Як один із варіантів оптимізації для покращення ефективності пристрою запропоновано ввести додатковий шар CdSeTe між шарами CdS та CdTe. Проаналізовано основні фотовольтаїчні параметри такого сонячного елементу в залежності від товщини шару CdSeTe та вмісту в ньому селену. Продемонстровано, що додавання твердого розчину CdSeTe в шар поглинача CdTe товщиною 1500 нм підвищує ефективність сонячного елемента на 6,84 %. Проведено порівняння основних фотовольтаїчних характеристик сонячних елементів CdS/CdTe та CdS/CdSeTe/CdTe. Отримані результати показали, що змодельована структура CdS/CdSeTe/CdTe забезпечує кращу ефективність фотоперетворення у світловому спектрі AM1.5G в порівнянні з класичною CdS/CdTe структурою. Такі елементи можуть використовуватися для формування високоефективних сонячних панелей.

Ключові слова: сонячний елемент, SCAPS, тонкі плівки, гетероструктури, телурид кадмію, халькогенід кадмію.

DOI: 10.15587/1729-4061.2024.313878

ОЦІНКА ПОТЕНЦІЙНОЇ ТОЧНОСТІ МАЛОГАБАРИТНОГО ГОНІОМЕТРА ІЗ РОЗШИРЕНИМ ДИНАМІЧНИМ ДІАПАЗОНОМ НА ОСНОВІ ЯДЕРНОГО МАГНІТНОГО РЕЗОНАНСУ (с. 13–25)

С. В. Іванов

Дослідження присвячено оцінці потенційних точнісних характеристик малогабаритного гоніометра на основі ядерного магнітного резонансу з розширеним динамічним діапазоном. Це потребувало отримання моделі похибок гоніометра, оцінки його точності на основі цієї моделі та формулювання практичних рекомендацій з розробки такого приладу на основі виконаної оцінки точності.

Для проведення оцінки точності ядерного гоніометра розроблено теоретичну модель, яка дозволяє визначити оптимальні робочі параметри газової суміші комірки, діапазони їх допустимих змін, чутливість гоніометра, залежність його характеристик від зовнішніх і внутрішніх факторів. Зокрема, визначено залежність вихідного сигналу приладу від параметрів газової суміші, оптичної накачки. Для гоніометра з коміркою об'ємом 8 см^3 оптимальна температура складає 130 °C, оптимальна інтенсивність випромінювання накачки 5 мВт.

Також визначено залежність вихідного сигналу від вимірюваного кута повороту, проаналізовано шуми та залежність похибки приладу за допустимими значеннями його параметрів. На основі розробленої моделі визначено параметри гоніометра з коміркою об'ємом 8 см3; гранична кутова чутливість такого гоніометра при повному придушенні технічних шумів складає $\delta\varphi_{sen}$=1.0 кут.сек. Найбільший вклад в похибку вимірювання кута вносить нестабільність потужності накачки I_p ($\Delta I_p/I_p$=0,05) – 85 %; магнітного поля B_0 ($\Delta B_0/B_0$=10^{-8}) – 13 %, температури T ($\Delta T/T$=0,1) – 2 %.

Розглянутий гоніометр відповідає середньому класу точності, $\delta\varphi_{tot}\geq$10 кут.сек. Він може знайти застосування в оптичному виробництві для оперативного контролю, атестації та паспортизації оптичних виробів. Для поліпшення кутової точності гоніометра потрібно підвищувати стабільність інтенсивності лазерного накачування.

Ключові слова: гоніометр, ядерний магнітний резонанс, газова комірка, оптичне накачування, котушка Гельмгольца, Ларморова частота.

DOI: 10.15587/1729-4061.2024.310360

РОЗРОБКА МЕТОДІВ МОНІТОРИНГУ ТА ОПТИМІЗАЦІЇ ПІДЗЕМНИХ ДРЕНАЖНИХ СИСТЕМ З ВИКОРИСТАННЯМ БЕЗДРОТОВИХ СЕНСОРНИХ МЕРЕЖ ТА УЛЬТРАШИРОКОСМУГОВИХ АНТЕН (с. 26–36)

Kabi Yelikbay, Pramod Kumar, Ruslan Kassym, Tansaule Serikov, Maxsat Orunbekov, Ainur Turdy, Marzhan Temirbekova, Arai Tolegenova, Akmaral Tlenshieva, Makbal Kassymova

Це дослідження зосереджено на оптимізації ультраширокосмугових (УШС) антен, які є критично важливими в сучасних системах зв'язку завдяки їх широкому діапазону частот (3,1–10,6 ГГц) і високим можливостям передачі даних. У дослідженні розглядається проблема оптимізації ключових параметрів антени, таких як зворотні втрати, пікове посилення та ефективність випромінювання, а також забезпечення енергоефективності та довговічності мережі. Традиційні методи оптимізації, такі як LEACH-C, часто не в змозі збалансувати ці фактори, що призводить до неоптимальної продуктивності.

Щоб вирішити цю проблему, було розроблено нейромережу Generalized Position-based Optimization Neural Network (GPON) для оптимізації УШС антени. Здійснено оцінку методу гібридної нейронної мережі на основі позиції (ПНМ), порівнявши його продуктивність з існуючими алгоритмами, включаючи LEACH-C, алгоритм Firefly, HFAPSO, FA-ANN і HWOABCA. Модель GPON зменшила зворотні втрати до 25,5 дБ на 3,5 ГГц і покращила пікове посилення до 4,2 дБ і, зберігаючи ефективність випромінювання на 92 %. Навпаки, PAN продемонстрував покращення залишкової енергії на 15–25 % і подовжив термін служби мережі на 20 % порівняно з LEACH-C.

Ці вдосконалення відбулися завдяки інтеграції передових методів нейронної мережі в GPON і ефективному використанню позиційних даних у ПНМ, що забезпечує більш точну та адаптивну оптимізацію. Здатність збалансувати декілька показників продуктивності одночасно – це проблема, з якою боролися попередні моделі – є ключовою особливістю. Цей баланс має вирішальне значення для УШС антен у системах зв'язку, де продуктивність та енергоефективність є життєво важливими. Висновки особливо актуальні для практичних застосувань у бездротових сенсорних мережах, мобільному зв'язку та радарних системах, що вимагають довгострокової надійності мережі та оптимальної продуктивності антени.

Ключові слова: ультраширокий діапазон, оптимізація антени, GPON, енергоефективність, довговічність мережі, нейронні мережі.

DOI: 10.15587/1729-4061.2024.309907

МОДЕЛЬ РОЗРОБКИ ВИСОКОЕФЕКТИВНОЇ МІКРОСМУЖКОВОЇ АНТЕНИ MIMO НА ОСНОВІ ПЛОСКОЇ ПОСЛІДОВНОЇ РЕШІТКИ З 8Ч2 ЕЛЕМЕНТАМИ ДЛЯ СИСТЕМ ЗВ'ЯЗКУ 5G (с. 37–49)

Syah Alam, Indra Surjati, Lydia Sari, Yuli Kurnia Ningsih, Suryadi, Teguh Firmansyah, Zahriladha Zakaria

Технологія MIMO (Multiple Input Multiple Output) здійснює значний внесок у розвиток систем зв'язку 5G зі збільшенням пропускної здатності мережі та ефективності використання спектру. У системах 5G технологія MIMO дозволяє використовувати кілька антен на базових станціях і пристроях користувачів, забезпечуючи одночасну відправку та прийом даних по декількох каналах. Це дозволяє значно підвищити пропускну здатність і надійність з'єднання, особливо у середовищах з високою щільністю користувачів. Крім того, технологія MIMO підтримує реалізацію технології формування діаграми спрямованості, яка фокусує сигнали в певному напрямку, знижує перешкоди й покращує покриття та якість сигналу, що робить її одним з ключових факторів для підвищення швидкодії та відгуку систем 5G. Таким чином, антени з широкою смугою пропускання, високим коефіцієнтом посилення та ефективністю MIMO мають вирішальне значення для підтримки систем зв'язку 5G. У даній роботі пропонується високоефективна мікросмужкова антена MIMO на основі послідовної плоскої решітки з 8×2 елементами, що працює на резонансній частоті 3,5 ГГц для систем зв'язку 5G. Для регулювання коефіцієнта відбиття та смуги пропускання антени пропонується використовувати спіральний шлейф і фідерну вставку, а для збільшення коефіцієнта посилення – послідовну плоску решітку. Для підтримки системи зв'язку MIMO запропонована антена розділена на два різних порти на певній відстані. Виходячи з результатів вимірювань, запропонована антена має високу ефективність,про що свідчить широка смуга пропускання 680 МГц (3–3, 68 ГГц) та високий коефіцієнт посилення 17,8 дБ за резонансної частоти 3,5 ГГц. Крім того, запропонована антена має високий взаємний зв'язок і рознесення, про що свідчать значення ECC і DG, які становлять 0,001 і 9,99 дБ відповідно. Дана робота представляє рішення для проектування високоефективної мікросмужкової антени, що може бути реалізована в якості приймальної антени для систем зв'язку 5G.

Ключові слова: мікросмужкова антена, високий коефіцієнт посилення, система MIMO, плоска антенна решітка, система 5G.

DOI: 10.15587/1729-4061.2024.313455

ОПТИМІЗАЦІЯ РОЗПОДІЛЕНИХ АКУСТИЧНИХ ДАТЧИКІВ НА ОСНОВІ ВОЛОКОННО-ОПТИЧНИХ ТЕХНОЛОГІЙ (с. 50–59)

Askar Abdykadyrov, Nurzhigit Smailov, Akezhan Sabibolda, Gulzhaina Tolen*, Zhandos Dosbayev, Zhomart Ualiyev, Rashida Kadyrova

Це дослідження досліджує розподілені акустичні датчики (РАД), засновані на волоконно-оптичних технологіях, зосереджуючись на впливі тиску на відношення сигнал/шум (ВСШ), рівні шуму та домінуючі зрушення частоти. Системи РАД широко використовуються для моніторингу інфраструктури завдяки своїй здатності фіксувати акустичні сигнали на великих відстанях, що робить їх ідеальними для сейсмічного моніторингу та моніторингу трубопроводів.

Дослідження вивчає, як коливання тиску впливає на продуктивність РАД, зокрема на якість сигналу та зменшення шуму. У таких програмах, як виявлення витоків у трубопроводі та сейсмічний моніторинг, зміни тиску можуть погіршити чіткість сигналу та ускладнити виявлення аномалій. Розуміння цього зв'язку є ключовим для оптимізації продуктивності РАД і підвищення ефективності системи.

Експеримент змінював тиск від 0,1 атм до 5 атм, показуючи, що підвищення тиску підвищило ВСШ з 10 дБ до 48 дБ, зменшило шум з 10 дБ до 7 дБ і зрушило домінуючу частоту з 0,5 Гц до 3 Гц. Аналіз Фур'є дав зрозуміти ці зміни частотного спектру. Більш високий тиск стискає середовище, покращуючи ізоляцію сигналу та покращуючи ВСШ, одночасно зменшуючи шум. Зсув частоти є результатом зміни швидкості поширення акустичної хвилі під високим тиском, підкреслюючи його роль в обробці сигналу.

Ключовий висновок полягає в тому, що вищий тиск значно покращує якість сигналу та зменшує шум, покращуючи продуктивність РАД. Зсув частоти покращує можливості виявлення навколишнього середовища. Ці результати є цінними для додатків РАД у

середовищах із коливаннями тиску, як-от моніторинг трубопроводів, де висока якість сигналу має вирішальне значення. Покращена точність сигналу та зрушення частоти роблять системи РАД більш надійними для тривалого моніторингу та сприяють точному виявленню аномалій.

Ключові слова: волоконно-оптичні технології, розподілені акустичні датчики, сейсмічний моніторинг, моніторинг інфраструктури.

DOI: 10.15587/1729-4061.2024.312489

ВИЗНАЧЕННЯ ХАРАКТЕРИСТИК КОНЦЕПТУАЛЬНОГО ПРОТОТИПУ МІКРОПРОЦЕСОРНОЇ РЕСУРСОЗБЕРІГАЮЧОЇ СИСТЕМИ РЕЛЕЙНОГО ЗАХИСТУ (с. 60–69)

Alexandr Neftissov, Ilyas Kazambayev, Lalita Kirichenko, Dnislam Urazayev, Andrii Biloshchytskyi, Omirzak Abdirashev

Об'єктом дослідження є концептуальний прототип мікропроцесорної ресурсозберігаючої системи релейного захисту. В даний час релейний захист забезпечує надійну й ефективну роботу електромереж, проте традиційна архітектура є запатентованою, що не дозволяє проводити ремонт та заміну пошкоджених деталей без участі фахівця компанії. Тому релейний захист із відкритою архітектурою є досить актуальним питанням, проте проблема полягає в дотриманні вимог до релейного захисту. Проведено оцінку протоколів передачі даних nRF та ESP-NOW, датчиків Холла для вимірювання величини змінного струму й підвищення точності датчиків. Експериментальна перевірка показала, що протоколи nRF та ESP-NOW відповідають вимогам щодо затримки та надійності, проте протокол nRF є більш підходящим завдяки своїй гнучкості та здатності подолання перешкод. Отримані дані показали, що найбільш ефективними умовами є відсутність перешкод на відстані 15 метрів від модему та наявність перешкод на відстані 5 метрів від модему. Експеримент з визначення характеристик датчиків Холла показав точність вимірювання струму при заданих значеннях струмів розмикання й замикання. Однак він не є точним (12,45 %) для застосування в релейному захисті. Тож застосування змінних значень струмів розмикання й замикання є більш ефективним, а точність досягає 6,92 %. В результаті було визначено термін служби датчика Холла, і навіть після 10 мільйонів розмикань час перебування в розімкнутому стані залишався незмінним. Таким чином, була знайдена апроксимуюча функція для визначення амплітуди струму в залежності від часу перебування в розімкнутому стані. З іншого боку, датчики Холла можуть страждати від температурного дрейфу й вимагають подальшої оптимізації для забезпечення повної надійності. Обмеженням дослідження є діапазон струму від 0 до 800 А.

Ключові слова: релейний захист, геркон, датчик Холла, магнітне поле, відкрита архітектура.

DOI: 10.15587/1729-4061.2024.313747

РОЗРОБЛЕННЯ МАТЕМАТИЧНИХ МОДЕЛЕЙ ТЕПЛОПРОВІДНОСТІ ДЛЯ ЕЛЕМЕНТІВ ПРИСТРОЇВ З ВКЛЮЧЕННЯМИ (с. 70–79)

В. І. Гавриш, Е. А. Джумеля, О. Д. Грицай, С. І. Качан, В. Ю. Майхер

Розглянуто процес теплопровідності для ізотропного середовища, що містить чужорідне напівнаскрізне включення, та нагрівається локально зосередженим тепловим потоком. Для встановлення температурних режимів ефективної роботи електронних пристроїв розроблено лінійну і нелінійну математичні моделі визначення температурного поля. Коефіцієнт теплопровідності неоднорідної конструкції подано як ціле, з використанням асиметричних одиничних функцій, що автоматично забезпечує умови ідеального теплового контакту на поверхнях стику матеріалів. Це приводить до розв'язування одного рівняння теплопровідності з розривними та сингулярними коефіцієнтами. Для лінеаризації нелінійної крайової задачі запроваджено лінеаризуючу функції. У замкнутому вигляді отримано аналітично-числові розв'язки лінійної і нелінійної крайових задач. Для термочутливого середовища вибрано лінійну температурну залежність коефіцієнта теплопровідності конструкційних матеріалів. У результаті отримано аналітично-числовий розв'язок, який визначає розподіл температури у цьому середовищі. На цій основі виконано числовий експеримент, результати якого графічно відображені та підтверджують адекватність розроблених математичних моделей реальному фізичному процесу.

Матеріалом пластини та включення виступають кремній та срібло. Отримані результати для цих матеріалів за лінійною і нелінійною моделлю відрізняються на 7 %. Незначна їх відмінність пояснюється тим, що значення температурного коефіцієнта теплопровідності є невеликими. Розроблені моделі дають змогу аналізувати наведені середовища щодо їх термостійкості. Унаслідок, стає можливим її підвищити, а конструкції захистити від перегрівання, яке може привести до виходу з ладу окремих вузлів та їх елементів і цілого електронного пристрою.

Ключові слова: термостійкість конструкції, чужорідне напівнаскрізне включення, ідеальний тепловий контакт, конвективний теплообмін.

DOI: 10.15587/1729-4061.2024.314117

РОЗРОБЛЕННЯ МЕТОДУ ВИЗНАЧЕННЯ КОЕФІЦІЄНТА ВОЛОГОПРОВІДНОСТІ ҐРУНТІВ ЗЕМЛЯНОГО ПОЛОТНА З УРАХУВАННЯМ ЄВРОПЕЙСЬКИХ ПІДХОДІВ І СТАНДАРТІВ (с. 80–89)

А. В. Бубела, Л. П. Бондаренко, Є. І. Кватадзе, В. В. Стьожка, А. В. Івко

Об'єктом досліджень є теоретико-методичні підходи до визначення коефіцієнта вологопровідності ґрунтів земляного полотна. Основний фокус роботи спрямований на врахування європейських підходів і стандартів при розробленні методу визначення коефіцієнта вологопровідності ґрунтів.

У ході досліджень розроблено метод визначення коефіцієнта вологопровідності ґрунтів K_1, що характеризує дифузійний рух води, через фільтраційний коефіцієнт K_0, розрахований відповідно до європейських вимог за даними лабораторних випробувань.

Запропонований метод базується на математичній моделі, отриманій на основі диференціального рівняння зміни вологості в ґрунті. Модель особлива тим, що на відміну від існуючих, рух води моделювався знизу вверх, що відображає процес вологонакопичення в нижніх шарах земляного полотна від ґрунтових вод або верховодки.

Отримано гарне узгодження математичної моделі з даними інших авторів (відносна похибка не перевищила 12.98 %).

В роботі отримано пряму залежність між коефіцієнтом вологопровідності ґрунтів K_1 і їх початковою вологістю W_0 та обернену залежність між K_1 і повною вологоємністю ґрунтів $W_{ПВ}$. Залежності отримано в діапазоні зміни початкової вологості ґрунту W_0 від 0.08 до 0.15 та $W_{ПВ}$ від 0.15 до 0.5. Встановлено, що значення коефіцієнта вологопровідності ґрунтів K_1 збільшуються від $4,64 \cdot 10^{-6}$ до $3,81 \cdot 10^{-5}$ м^2/год при збільшенні їх початкової вологості та при зменшенні повної вологоємності.

З точки зору інженерної практики дорожнього будування, запропонований метод дає можливість прогнозувати сезонні зміни вологості ґрунтів земляного полотна, визначати міцність дорожньої конструкції. Це дозволяє приймати обґрунтовані проєктні рішення щодо влаштування дренажних систем на автошляхах задля подовження строку їх експлуатування.

Ключові слова: вологість ґрунту, коефіцієнт вологопровідності ґрунту, земляне полотно, дорожня конструкція.

DOI: 10.15587/1729-4061.2024.313114

ВИЗНАЧЕННЯ РОБОЧИХ ХАРАКТЕРИСТИК СИСТЕМИ ПІДПОРУ ПОВІТРЯ В АВАРІЙНОМУ ЛЮКУ НА БАЗІ СТРУМИННИХ ВОДОГАЗОВИХ ЕЖЕКТОРІВ (с. 90–99)

С. О. Гринчак

Об'єктом досліджень є струминні водогазові ежектори в системі забезпечення протипожежної безпеки кораблів. Проблема, що вирішувалася, – при пожежі в районі виходу з аварійного приміщення судна небезпечно підвищується теплова енергія і велика кількість диму поширюється по приміщеннях судна. Ці чинники вимагають негайної герметизації аварійного приміщення, що обмежує оперативний доступ аварійних команд в приміщення. Встановлення системи місцевого підпору повітря в аварійному люку на базі струминних водогазових ежекторів дозволить екранувати теплову енергію і локалізувати димові гази в аварійному приміщенні без його герметизації для забезпечення оперативного доступу аварійних команд до нього. Досягнуті наступні основні результати – підтверджено експериментальним методом адекватність теоретичних досліджень процесів локалізації димових газів в аварійному приміщенні без його герметизації. Досліджувана проблема була вирішена шляхом оптимізації процесів: швидкості зміни натурального показника послаблення середовища під час запуску місцевої системи підпору повітря в аварійному люку на базі струминних водогазових ежекторів; ефективності зниження температури нагрітих газів в надбудові при роботі системи підпору повітря в аварійному люку на базі струминних водогазових ежекторів. Особливістю отриманих результатів стало формування повітряної завіси, отриманої шляхом відбору частини високотемпературних димових газів у корпуси струминних водогазових ежекторів, їх тепломасообмінної обробки та виводу назад у потік. Це створило умови, при яких екранування теплової енергії відбувається з ефективністю 85–88 %. Сфера та умови практичного використання отримані результатів – суднобудування та проєктування протипожежної суднової безпеки.

Ключові слова: водогазовий струминний ежектор, аварійний люк, натуральний показник послаблення середовища, теплова енергія.

MIMO (Multiple Input Multiple Output) makes a major contribution to 5G communication systems by increasing network capacity and spectrum efficiency. In 5G, MIMO enables the use of multiple antennas at base stations and user devices, allowing simultaneous sending and receiving of data over multiple paths. This significantly increases data throughput and connection reliability, especially in environments with high user density. In addition, MIMO technology supports the implementation of beamforming, which focuses signals on a specific direction, reduces interference, and improves signal coverage and quality, making it one of the keys to achieving faster and more responsive 5G performance. Therefore, antennas with wide bandwidth, high gain and MIMO performance are crucial for supporting 5G communication systems. This paper proposes a high-performance MIMO microstrip antenna based on a series planar array with 8×2 elements operating at a resonant frequency of 3.5 GHz for 5G communication systems. A spiral stub and a feed inset are proposed to control the reflection coefficient and bandwidth of the antenna while the series planar array is proposed to increase the gain. To support the MIMO communication system, the proposed antenna is separated into two different ports with a certain distance. From the measurement results, the proposed antenna has high performance indicated by a wide bandwidth of 680 MHz (3–3.68 GHz) and a high gain of 17.8 dB at a resonant frequency of 3.5 GHz. In addition, the proposed antenna has high mutual coupling and diversity indicated by ECC and DG of 0.001 and 9.99 dB, respectively. This work provides a solution to design a high-performance microstrip antenna and can be implemented as a receiving antenna for 5G communication systems

Keywords: microstrip antenna, high gain, MIMO system, planar array, 5G system

UDC 621
DOI: 10.15587/1729-4061.2024.309907

DEVELOPMENT MODEL OF A HIGH-PERFORMANCE MULTIPLE INPUT MULTIPLE OUTPUT MICROSTRIP ANTENNA BASED ON A PLANAR SERIES ARRAY WITH 8×2 ELEMENTS FOR 5G COMMUNICATION SYSTEMS

Syah Alam
Corresponding author
Doctor of Electrical Engineering, Associate Professor, Lecture*
E-mail: syah.alam@trisakti.ac.id
Indra Surjati
Doctor of Electrical Engineering, Professor, Lecture*
Lydia Sari
Doctor of Electrical Engineering, Associate Professor, Lecture*
Yuli Kurnia Ningsih
Doctor of Electrical Enginnering, Associate Professor, Lecture*
Suryadi Suryadi
Bachelor of Electrical Enginnering, Assistant Professor, Lecture*
Teguh Firmansyah
Doctor of Electrical Engineering, Lecturer
Department of Electrical Engineering
Universitas Sultan Ageng Tirtayasa
Ciwaru Raya str., 25, Serang, Banten, Indonesia, 42117
Zahriladha Zakaria
Doctor of Electrical Engineering, Professor
Faculty of Electronic Engineering and Computer Engineering (FKEKK)
Universiti Teknikal Malaysia Melaka (UTeM)
Hang Tuah Jaya str., Durian Tunggal, Melaka, Malaysia, 76100
*Department of Electrical Engineering
Universitas Trisakti
Kyai Tapa str., 1, DKI Jakarta, Indonesia, 11440

Received date 15.07.2024
Accepted date 25.09.2024
Published date 30.10.2024

***How to Cite:** Alam, S., Surjati, I., Sari, L., Ningsih, Y. K., Suryadi, S., Firmansyah, T., Zakaria, Z. (2024). Development model of a high-performance multiple input multiple output microstrip antenna based on a planar series array with 8×2 elements for 5G communication systems. Eastern-European Journal of Enterprise Technologies, 5 (5 (131)), 37–49. https://doi.org/10.15587/1729-4061.2024.309907*

1. Introduction

5G communication systems require more sophisticated and diverse antennas than previous generations to support various technological advancements, such as MIMO and millimeter wave (mmWave) [1–3]. MIMO (Multiple Input Multiple Output) is a technology that plays a key role in 5G communication systems. The main advantage of MIMO in 5G is its ability to significantly increase capacity and data rates without requiring more frequency spectrum. By using multiple antennas on the transmit and receive side, MIMO allows simultaneous data transmission over multiple paths, reducing interference and increasing spectral efficiency [4, 5]. In addition, MIMO can improve signal coverage and reliability by using techniques such as beamforming, which focuses the signal toward a specific user. This is especially important in delivering a faster and more stable experience for users in sub-urban areas [6]. According to [7], the resonant frequency for 5G communication systems is categorized into three bands: high, middle, and low. One of the recommended frequencies for 5G communication systems is 3.5 GHz, which is included in the middle band category and dynamic environments, such as urban or high-mobility areas [8].

Furthermore, microstrip antennas offer several important advantages for 5G applications, particularly in terms of integration, size, and performance [9, 10]. Due to their thin and lightweight design, microstrip antennas can be easily integrated into portable devices such as smartphones and IoT devices, as well as into network infrastructure such as base stations [11, 12]. They can also be manufactured in arrays, enabling the implementation of MIMO and beamforming technologies, which are essential for increasing the capacity and transmission speed in 5G networks [13, 14]. In addition, microstrip antennas can be designed to operate at a wide range of frequencies, including high frequencies such as mmWave used in 5G, while maintaining good efficiency. Their relatively low production costs and ability to be printed on a variety of substrates also make them an economical and practical choice for widespread 5G deployment. However, microstrip antennas have certain drawbacks, such as narrow bandwidth, low gain, and limited directivity. The primary parameters that indicate an antenna's performance include the reflection coefficient, bandwidth, gain, and radiation pattern. Therefore, antennas with wide bandwidth and high gain are crucial for supporting wireless communication systems such as Wi-Fi, 4G, and 5G. Moreover, high-performance antennas with multiple input multiple output are essential to facilitate communication between the transmitter and receiver, especially for 5G communication systems.

2. Literature review and problem statement

Several previous studies have explored and proposed microstrip antennas for 5G communication systems using various techniques, including fractal designs, arrays, and parasitic elements. Furthermore, in a study presented by [10], microstrip antennas with wider bandwidths were achieved by incorporating parasitic elements placed above the radiating elements. However, the antenna's gain remained low, necessitating further improvement. Previous work [15] proposed a fractal antenna for 5G communication with MIMO configuration operating at a resonant frequency of 3.5 GHz. However, the gain of the proposed antenna is still low at about 3 dB. Another work [16] proposed a ten-element MIMO array antenna that operates at a resonant frequency of 3.5 GHz. However, the bandwidth of the proposed antenna is still low at about 200 MHz. Moreover, the previous work [17] presented a wideband microstrip antenna operating at a resonant frequency of 3.35–3.95 GHz with a 2×2 element MIMO array. However, the gain of the proposed antenna is only 12.6 dB. Another study by [18] proposed a microstrip antenna array with four elements operating at a resonant frequency of 3.5 GHz, achieving a bandwidth of 0.7 GHz and a gain of 9.24 dB. Nevertheless, the increase in bandwidth was accompanied by a decrease in gain, indicating an inverse relationship between bandwidth and gain. In addition, previous work by [19] proposed a microstrip antenna using an array with 4×2 elements with a bandwidth of 0.6 GHz and a gain of 12.2 dB. However, the proposed antenna does not support MIMO communication systems. Other findings describe MIMO microstrip antennas based on vertical and horizontal configurations with 2 ports operating at resonant frequencies of 3.5 GHz and 6 GHz [20]. However, the gain obtained is still low at around 7.8 dB. Based on the literature review [15–20], the limitation of previous works is that the proposed antenna still has low gain, narrow bandwidth and does not support MIMO. Therefore, an antenna with wide bandwidth, high gain and MIMO support is needed as a solution for receivers in 5G communication systems. In addition, MIMO technology supports the implementation of beamforming, which focuses signals on a specific direction, reduces interference, and improves signal coverage and quality, making it one of the keys to achieving faster and more responsive 5G performance.

3. The aim and objectives of the study

The aim of the study is to propose an antenna configured with two different ports separated by a certain distance in order to support MIMO capabilities.

To achieve this aim, the following objectives are accomplished:

– to produce a design and model of a microstrip antenna that operates at a resonance frequency of 3.5 GHz with a bandwidth of 200 MHz for a 5G communication system;

– to produce a design and model of a microstrip antenna with a high gain ≥12 dB that operates at a frequency of 3.5 GHz for a 5G communication system;

– to validate and measure microstrip antennas that can be used in MIMO communication systems with low mutual coupling $S_{21}\leq-20$ dB.

4. Materials and methods

The object of the study is 5G communication systems. The main hypothesis of the study is as follows. A high-performance MIMO microstrip antenna based on a series planar array with 8x2 elements operating at a resonant frequency of 3.5 GHz; will improve the capabilities of 5G communication systems.

The proposed antenna is designed using an FR-4 substrate with a dielectric constant of 4.3, tan delta of 0.0265 and thickness of 1.6 mm. The radiation element of the antenna is represented by a rectangular patch placed on the top layer of the substrate while the bottom layer functions as a ground plane. The antenna is connected directly with a brass connector using a microstrip line with an impedance of 50 ohms. The evolution and models of the proposed antenna are shown in Fig. 1. The antenna is designed and simulated using EM simulation based on HFSS 15.0.

Fig. 1 shows that the proposed antenna is developed in six models. Model 1 proposes an antenna with a single element that operates at a resonance frequency of 3.5 GHz, which is represented in Fig. 1, *a*. Furthermore, model 2 and model 3 propose two-element and four-element array antennas based on a series configuration with a spiral stub shown in Fig. 1, *b*, *c*.

Model 4 proposes an eight-element array antenna by adding an inset fed to the antenna patch while model 5 proposes an array antenna with 8×2 elements configured based on the horizontal planar shown in Fig. 1, *d*, *e*. The last model proposes an array antenna with 8×2 elements configured as MIMO using two ports separated by a certain distance represented by Fig. 1, *f*. The addition of the spiral stub and fed inset aims to reduce the reflection coefficient while adding the number of elements on the array antenna aims to increase the gain.

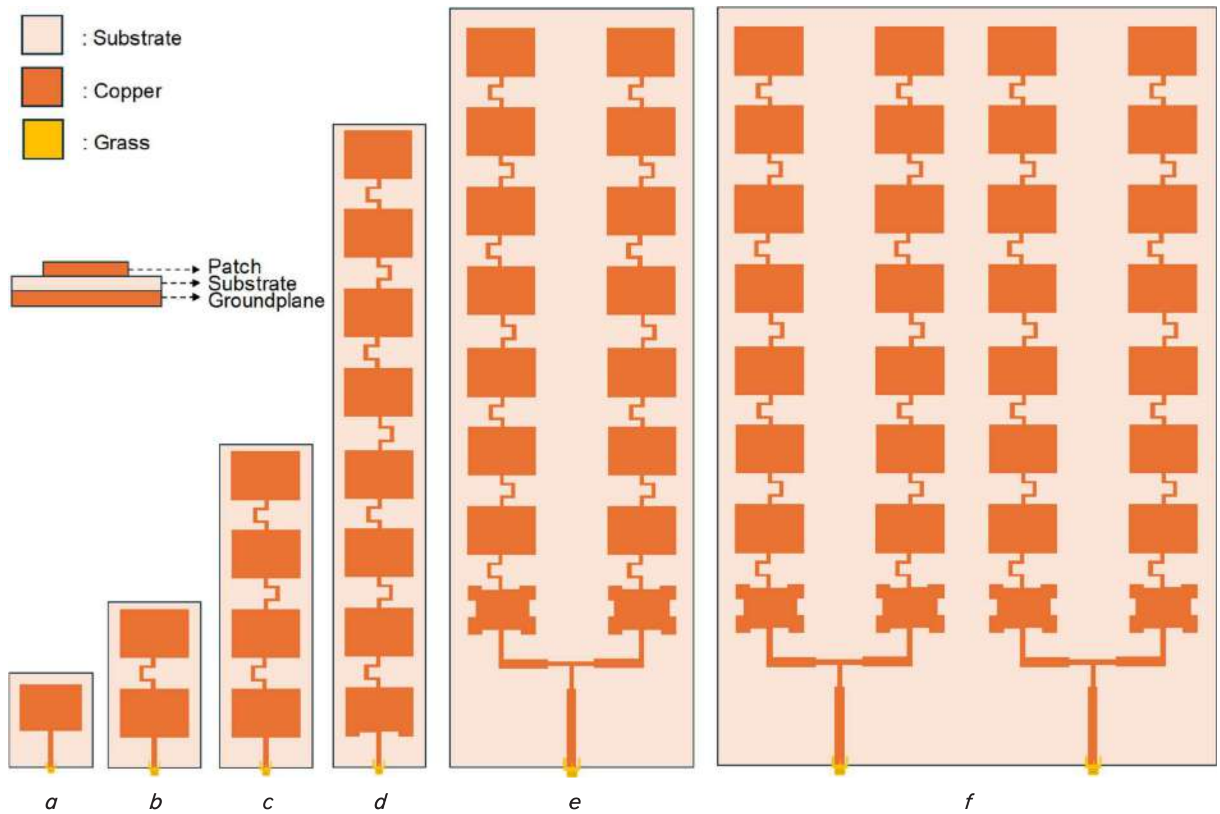

Fig. 1. Evolution of the proposed antenna: *a* – single-element; *b* – 2-element array; *c* – 4-element array; *d* – 8-element array; *e* – 8×2 element planar array; *f* – MIMO planar array

5. Results of the design and realization of the proposed antenna

5. 1. Design of a series array antenna

At the first stage, the antenna is designed with a rectangular patch to operate at a resonant frequency of 3.5 GHz. The length and width of the antenna patch are represented respectively by W_p and L_p, which are determined based on the following equation [21]:

$$W_p = \frac{c}{2f_o\sqrt{\frac{\varepsilon_r}{2}}}, \quad (1)$$

$$L_p = L_{eff} - \Delta_L, \quad (2)$$

$$L_{eff} = \frac{c}{2f_o\sqrt{\varepsilon_{eff}}}, \quad (3)$$

$$\varepsilon_{eff} = \frac{\varepsilon r+1}{2} + \frac{\varepsilon r-1}{2}\left[1+12\frac{h}{W}\right]^{-\frac{1}{2}}, \quad (4)$$

$$\Delta_L = 0.412\frac{(\varepsilon_{reff}+0.3)\left(\frac{W}{h}+0.264\right)}{(\varepsilon_{reff}-0.258)\left(\frac{W}{h}+0.8\right)}. \quad (5)$$

In this context, W_p and L_p denote the width and length of the patch, respectively; f_o signifies the resonance frequency, ε_r indicates the substrate's permittivity, ε_{eff} refers to the effective permittivity of the substrate at a specific resonance frequency, h stands for the substrate's thickness, and Δ_L accounts for the fringing field's edge effect on the patch. In addition, microstrip lines are suggested for managing the impedance and reflection coefficient of the antenna. The size of the microstrip line is significantly affected by the input impedance and the chosen resonant frequency. In this study, the input impedance is set to 50 ohms. The dimensions of the microstrip line can be calculated using the following equation [22]:

$$W_z = \frac{2h}{\pi}\left\{\begin{matrix} B-1-\ln(2B-1)+ \\ +\frac{\varepsilon_r-1}{2\varepsilon_r}\left[\ln(B-1)+0.39-\frac{0.61}{\varepsilon_r}\right]\end{matrix}\right\}, \quad (6)$$

$$B = \frac{60\pi^2}{Z_0\sqrt{\varepsilon_{eff}}}. \quad (7)$$

In this context, W_z represents the width of the microstrip line, π is constant, Z_o denotes the antenna's impedance, and B stands for the impedance constant. The antenna's impedance is 50 Ω, matching the impedance of the connector used. Additionally, the length of the microstrip line (L_z) is ¼ of the wavelength (λ_g), calculated using the following equation [21]:

$$L_z = \frac{1}{4}\lambda_g, \quad (8)$$

$$\lambda_g = \frac{\lambda}{\varepsilon_{eff}}. \quad (9)$$

The structure and simulation results of an antenna with a single element are shown in Fig. 2.

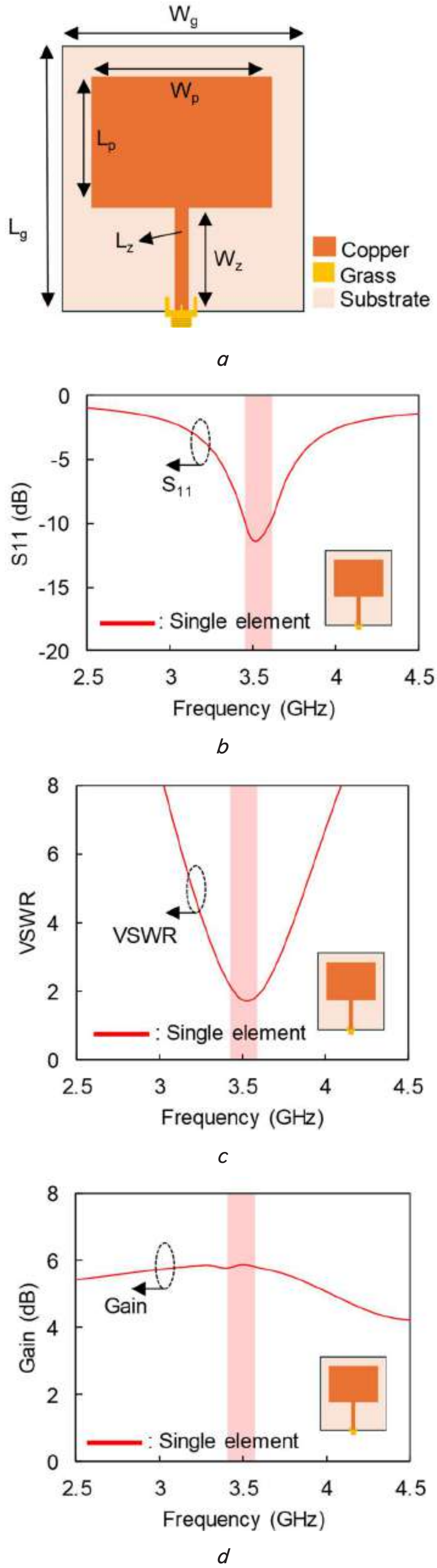

Fig. 2. Model of a single-element antenna: *a* – design of a single element; *b* – simulation of S_{11}; *c* – simulation of VSWR; *d* – simulation of gain

Fig. 2, *a* shows the dimensions of W_p and L_p being 26 mm and 22 mm, respectively. In addition, the length and width of the microstrip lines represented by L_z and W_z are 13 mm and 3 mm. The dimensions of the ground plane are shown by W_g and L_g where the width and length are 35 mm and 29 mm. Furthermore, the simulation results of S_{11}, VSWR in Fig. 2, *a*, *b* show that the antenna has been operating at a resonance frequency of 3.5 GHz with S_{11} –11.34 dB and VSWR 1.74. The gain of the single-element antenna is shown in Fig. 2, *c* where the peak gain at a resonance frequency of 3.5 GHz is 5.8 dB. However, the bandwidth obtained from the single-element antenna is still narrow at 40 MHz (3.48–3.52 GHz). Therefore, optimization is required to increase the bandwidth of the proposed antenna.

The second stage is to optimize the single-element antenna into a series array antenna with two elements. The purpose of adding elements is to increase the gain while the bandwidth of the antenna is optimized with a spiral-shaped stub. The structure and simulation results of an array antenna with two elements are shown in Fig. 3.

Fig. 3, *a* shows the structure of an array antenna with two elements, where the dimensions of W_g and L_g are 32 mm and 71 mm. Moreover, spiral stubs are proposed to connect between elements with lengths L_1, L_2 and L_3 of 6 mm, 7 mm and 6 mm. Furthermore, the width of the spiral stub is represented by W_b and W_s where the width is 3 mm and 1 mm, respectively. The simulation results of S_{11} and VSWR for an array antenna with two elements are shown in Fig. 3, *b*, *c* where S_{11} is –16.79 dB and VSWR is 1.33 at a resonance frequency of 3.5 GHz. The bandwidth obtained from the antenna array with two elements is 400 MHz (3.2–3.6 GHz) with a peak gain of 7.82 dB. This finding shows that the spiral stub and the addition of elements succeed in increasing the bandwidth and gain of the proposed antenna. However, the gain obtained is still low so further optimization is required. Therefore, the gain of the proposed antenna is optimized by increasing the number of elements of the array.

The third stage is to increase the antenna gain by optimizing the antenna array into four elements. The structure and simulation results of an array antenna with four elements are shown in Fig. 4.

Fig. 4, *a* illustrates the design of a four-element array antenna, with W_g and L_g of 32 mm and 142 mm, respectively. The array elements are linked by spiral stubs that extend in opposite directions. Furthermore, the simulation of S_{11} and VSWR shows that the antenna has high performance with S_{11} and VSWR of –29.28 dB and 1.07 at a resonance frequency of 3.5 GHz as shown in Fig. 4, *b*, *c*. The bandwidth obtained from the antenna array with four elements is 300 MHz (3.3–3.6 GHz) with a peak gain of 9.9 dB at a resonance frequency of 3.5 GHz as illustrated in Fig. 4, *d*.

The fourth stage is to optimize the antenna array with eight elements to increase the gain. Furthermore, an inset feed is proposed to control the resonant frequency of the antenna represented by W_i and W_d with dimensions of 7 mm and 1 mm, respectively. The length and width of the ground plane represented by W_g and L_g are 32 mm and 310 mm as shown in Fig. 5, *a*.

The simulation of S_{11} and VSWR of the array antenna with eight elements illustrated in Fig. 5, *b*, *c* shows that the antenna has been operating at a resonance frequency of 3.5 GHz with S_{11} of –26.37 dB and VSWR of 1.10. The bandwidth obtained is 300 MHz (3.3–3.6 GHz) while the peak gain is 10.82 dB at a resonance frequency of 3.5 GHz as shown in Fig. 5, *d*. Furthermore, the simulation results of S_{11} and the gain of the entire antenna model shown in Fig. 6, *a*, *b* are proposed to evaluate the optimization of the proposed antenna, respectively.

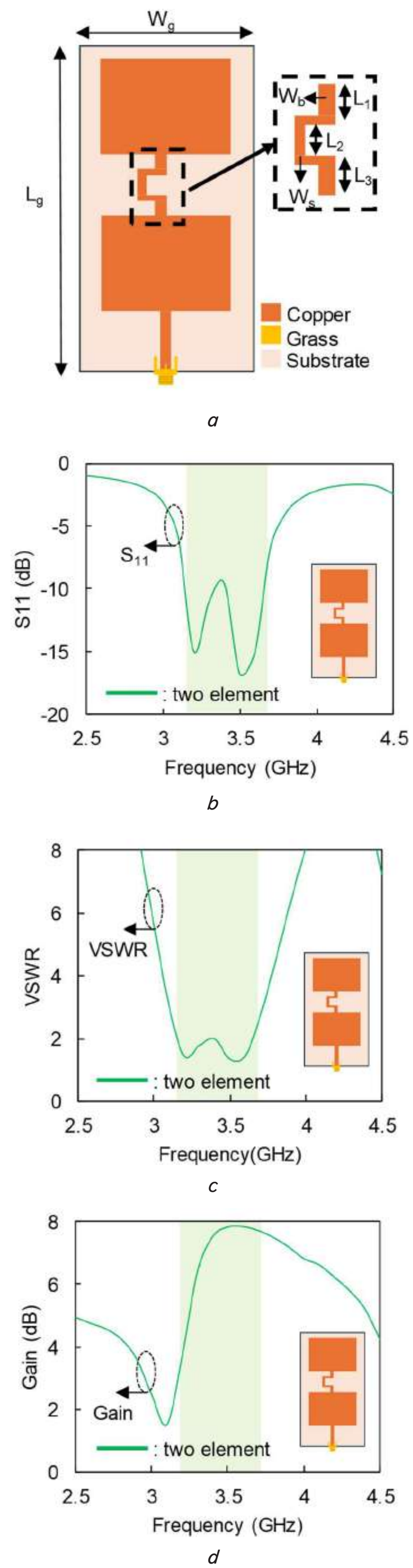

Fig. 3. Model of an array antenna with two elements: *a* — design of a two-element array with a spiral stub; *b* — simulation of S_{11}; *c* — simulation of VSWR; *d* — simulation of gain

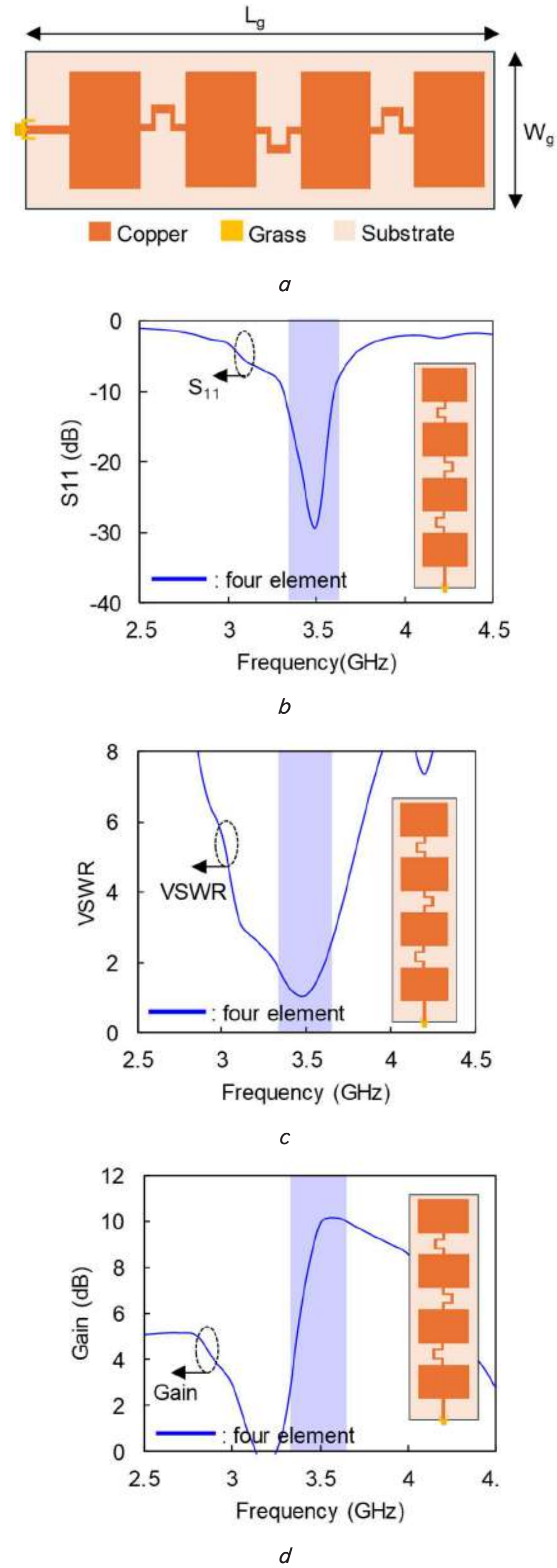

Fig. 4. Model of an array antenna with four elements: *a* — design of a four-element array with a spiral stub; *b* — simulation of S_{11}; *c* — simulation of VSWR; *d* — simulation of gain

Fig. 6, *a* illustrates that the reflection coefficient of the proposed antenna gradually improves from –11.23 dB to –26.27 dB at a resonance frequency of 3.5 GHz. This result indicates that the optimization using an eight-element array antenna, spiral stub, and inset feed effectively enhanced the antenna's performance in terms of the reflection coefficient by up to 134 % compared to a single-element antenna.

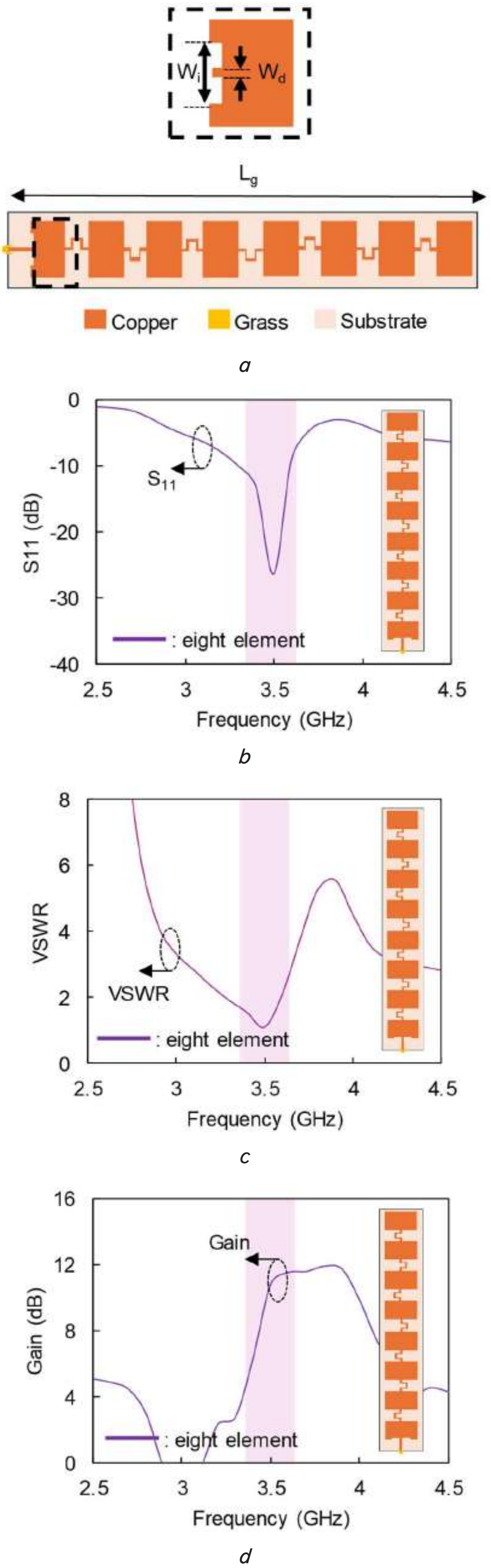

Fig. 5. Model of an array antenna with eight elements: *a* – design of an eight-element array with a spiral stub and inset fed; *b* – simulation of S_{11}; *c* – simulation of VSWR; *d* – simulation of gain

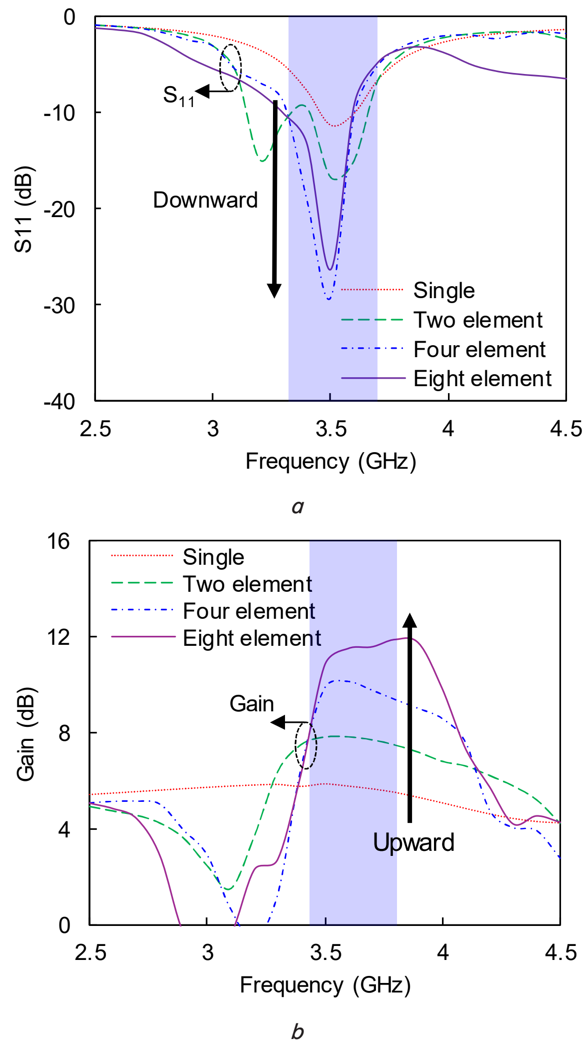

Fig. 6. Comparison of simulation results: *a* – simulation of S_{11}; *b* – simulation of gain

Additionally, the bandwidth of the proposed antenna expanded by 650 %, from 40 MHz (3.48–3.52 GHz) to 300 MHz (3.3–3.6 GHz). This demonstrates that the proposed antenna meets the specifications for the 5G communication system operating within the 3.4–3.6 GHz frequency range. Moreover, Fig. 6, *b* shows that the antenna's gain increases as the number of elements in the antenna array is increased, with a gain improvement of 78 % from 5.8 dB to 10.82 dB at a resonance frequency of 3.5 GHz.

However, the gain of the proposed antenna remains below the desired target ≥12 dB. Thus, additional optimization is necessary to enhance the antenna's gain.

5. 2. Design of a MIMO series planar array antenna with 8x2 elements

In order to increase the gain, the antenna is configured as a series planar array with 8×2 elements. The elements of the antenna array are connected with impedance matching based on T-stubs while the antenna elements are optimized with slits on the right and left edges of the patch. The structure of the series planar array antenna and the simulation results are shown in Fig. 7.

Fig. 7, *a* shows the elements of the antenna separated by a certain distance represented by d_a=21 mm, which is determined based on the following equation [22]:

$$d_a = \frac{1}{8}\lambda, \quad (10)$$

$$\lambda = \frac{c}{f}, \quad (11)$$

where d_a is the distance between elements, λ is the wavelength of the antenna and c is the speed of light (3×10^8 m/s). It should be noted that the distance between the elements of a planar array antenna greatly affects the gain. Furthermore, microstrip lines with stepped impedance are used as impedance matching between elements of the antenna array represented by Z_1=50 Ω, Z_2=70.7 Ω and Z_3=100 Ω. The width of the transmission line dictates its impedance, which can be calculated using the following equation [21]:

$$Z_2 = \sqrt{Z_1 \cdot Z_3}. \quad (11)$$

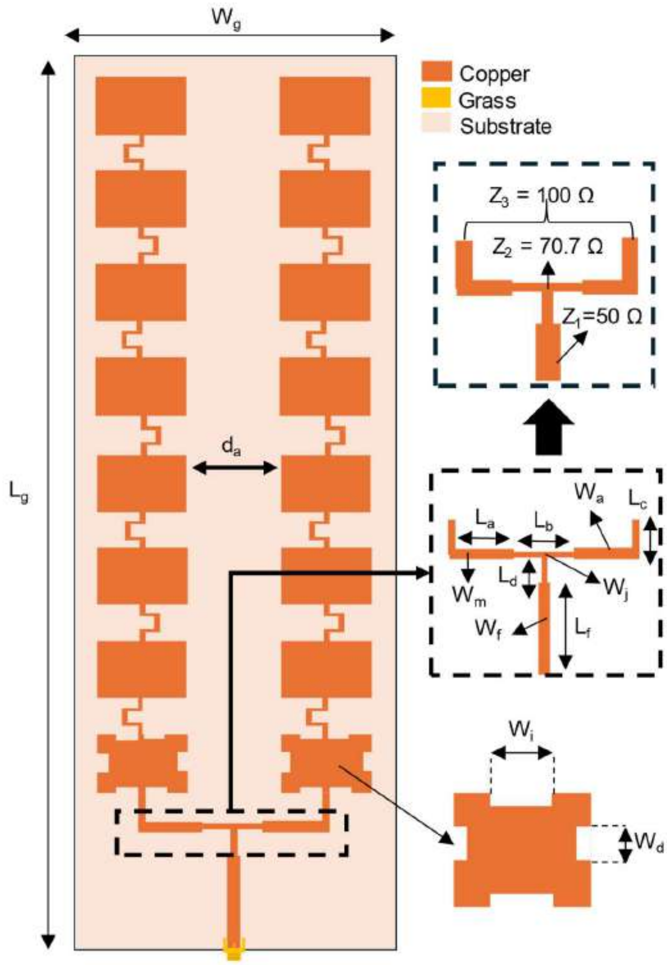

a

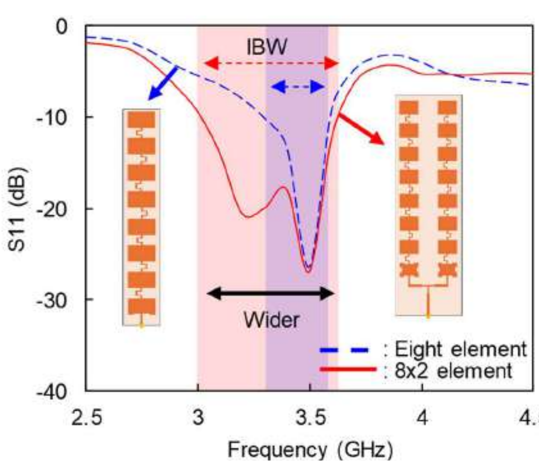

b

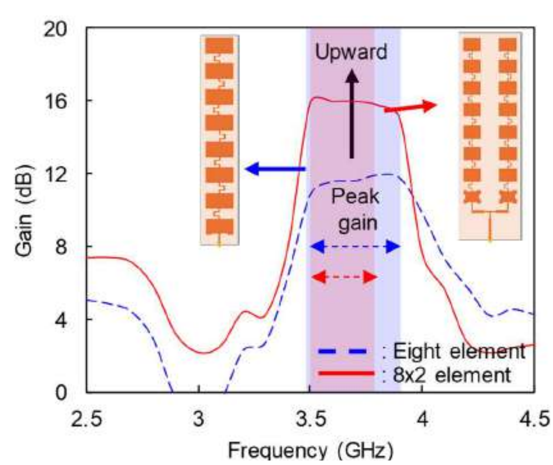

c

Fig. 7. Model of a series planar array antenna: *a* — design of an 8×2 element planar array with a spiral stub and inset fed; *b* — simulation of S_{11}; *c* — simulation of VSWR; *d* — simulation of gain

The width of the microstrip line with stepped impedance is represented by W_f=3 mm, W_j=1 mm and W_m=2 mm while the length is represented by L_f=33 mm, L_d=8 mm, L_b=23 mm, L_a=12 mm and L_c=17 mm. The dimensions of the ground plane indicated by W_g and L_g are 82 mm and 353 mm, respectively. Furthermore, Fig. 7, *b* shows that the bandwidth of the proposed antenna increases from 300 MHz (3.3–3.6 GHz) to 600 MHz (3–3.6 GHz). In addition, the peak gain of the antenna also increases from 10.82 to 16.09 dB at a resonant frequency of 3.5 GHz as shown in Fig. 7, *c*. These findings indicate that the proposed antenna has met the specifications for a 5G communication system with a bandwidth of ≤200 MHz and a gain of ≥12 dB at a resonant frequency of 3.5 GHz.

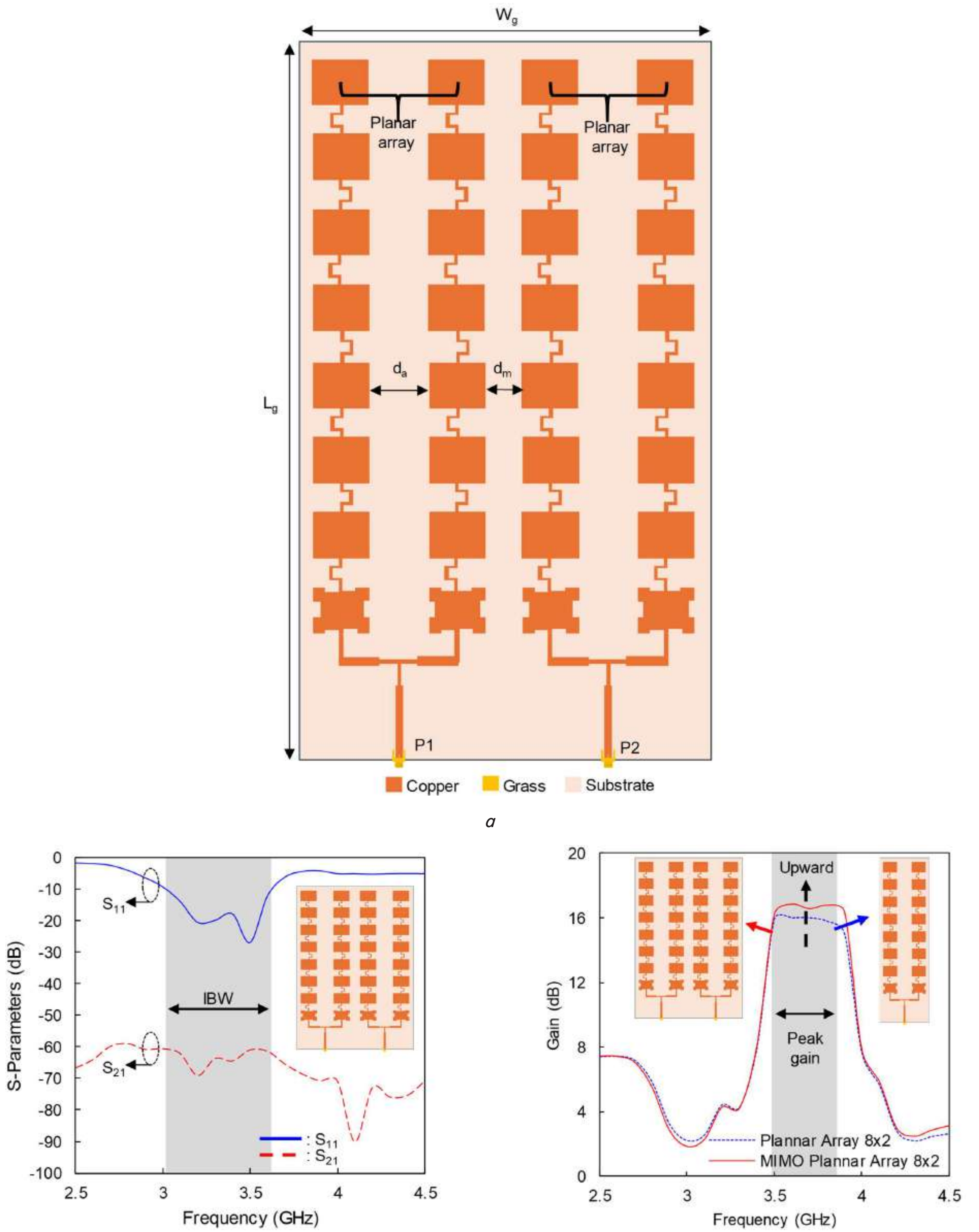

Fig. 8. Model of a MIMO series planar array antenna: *a* – design of an 8×2 element MIMO planar array; *b* – simulation of S_{11}; *c* – simulation of VSWR; *d* – simulation of gain

The next step is to optimize the antenna with a MIMO configuration that is directly connected to port 1 and port 2, respectively. It should be noted that the distance between the antennas at each port greatly affects the mutual coupling of the MIMO configuration. Mutual coupling shows the independence of the antennas when both works simultaneously. The minimum standard for mutual coupling is S_{21}≤–20 dB at the specified resonant frequency.

Furthermore, to support the 5G communication system, the antenna is configured in MIMO with 2 different ports represented by port 1 (P1) and port 2 (P2) as shown in Fig. 8, *a*. The structure of the series planar antenna array is connected to P1 and P2, respectively. In order to control the independence of the two antennas with high mutual coupling, the antennas are separated by a certain distance represented by d_m=21 mm. The dimensions of the ground plane are represented by W_g and L_g, which are 164 mm and 353 mm, respectively.

The simulation results illustrated in Fig. 8, *b* show that the antenna has been operating at a resonant frequency of 3.5 GHz with S_{11} and S_{21} around –20 dB and –60 dB with a bandwidth of 650 MH (3–3.65 GHz). This finding indicates that the antenna has a bandwidth that meets the criteria for the 5G communication system and has high mutual coupling with S_{21}≤–20 dB. In addition, the gain of the antenna with MIMO configuration also increases from 15.98 dB to 16.78 dB as shown in Fig. 8, *c*. This shows that the proposed antenna has met the specifications for 5G communication systems where the gain is ≥12 dB. The next stage is to fabricate and validate the performance of the proposed antenna through a measurement process in the laboratory.

5. 3. Validation and measurement of the proposed antenna

The antenna is fabricated using an FR-4 substrate where the radiating element is located on the top layer while the bottom layer functions as a ground plane as shown in Fig. 9, *c*. Validation of the near-field performance is carried out through a measurement process using a Vector Network Analyzer (VNA) with a frequency range of 2.5–4.5 GHz, a frequency step size of 0.01 GHz and a temperature of 25°, which is connected to the antenna (AUT) via port 1 and port 2 with a coaxial cable as shown in Fig. 9, *a*.

The measurement setup consists of an antenna under test (AUT), which functions as a transmitter (*Tx*) connected to an *RF* generator while a reference antenna is placed as a receiver (*Rx*) connected to a spectrum analyzer and separated based on the Fresnel zone where d_f=2D^2/λ [20]. The antenna is placed on a rotator that rotates clockwise from 0–360° with a step size of 1°. The far-field characteristics of the proposed antenna are observed based on the antenna's radiation pattern when transmitting and receiving electromagnetic waves.

A comparison of the simulation and measurement results of S_{11} and S_{21} in Fig. 10, *a* show that the fabricated antenna has the same performance as the simulated antenna where S_{11} is around –20 dB while S_{21} is around –40 dB at a resonance frequency of 3.5 GHz. The bandwidth of the fabricated antenna is 680 MHz with a frequency range of 3–3.68 GHz. This finding shows that the measurement results are in line with the simulation results.

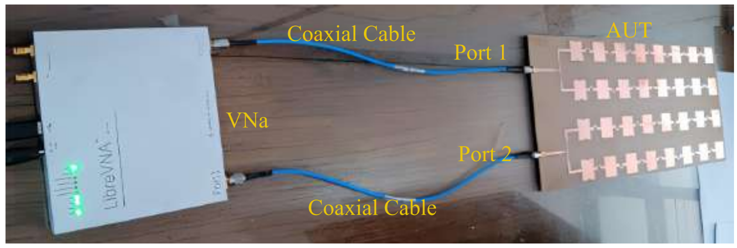

a

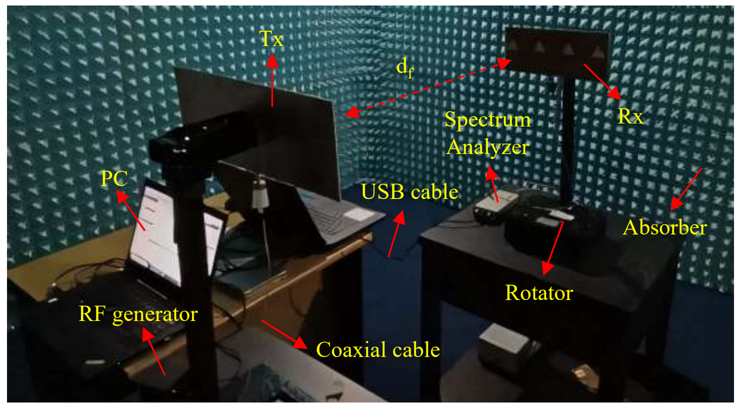

b

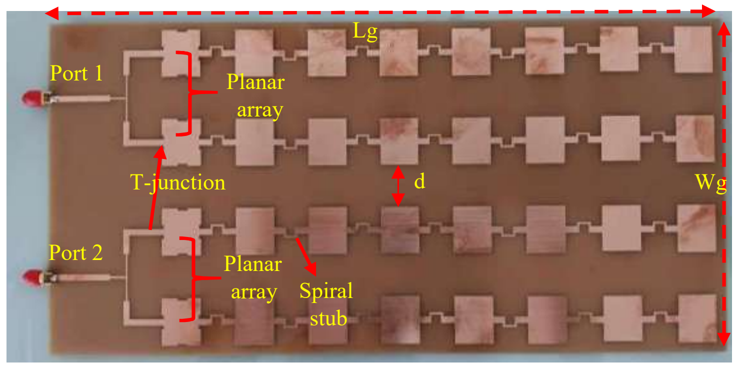

c

Fig. 9. Measurement process of the proposed antenna: *a* – measurement setup for near-field validation; *b* – measurement setup for far-field validation in an anechoic chamber; *c* – fabrication of the proposed antenna

The subsequent phase involves assessing the performance of the MIMO antenna by examining the Envelope Correlation Coefficient (ECC) and Diversity Gain (DG) parameters. The ECC quantifies the correlation between the two antennas operating in tandem within a MIMO configuration. Typically, the ECC value lies within the range of 0 to 1, with a threshold of ≤0.5 generally accepted for MIMO antenna designs. The ECC can be calculated using the following equation [20]:

$$ECC = \frac{\left|S_{11}^{*}S_{12} + S_{21}^{*}S_{22}\right|^{2}}{\left(1-\left|S_{11}\right|^{2}-\left|S_{21}\right|^{2}\right)-\left(1-\left|S_{22}\right|^{2}-\left|S_{12}\right|^{2}\right)}. \quad (12)$$

Diversity Gain (DG) characterizes the capability of an antenna system to mitigate the effects of multipath fading.

The DG value reflects the system's ability to enhance or sustain the signal quality relative to noise by combining signals from multiple antennas rather than relying on a single antenna. For MIMO antennas, the diversity is typically represented by a DG value of ≤10 dB [18]. The DG can be calculated using the following equation [20]:

$$DG = 10\sqrt{1-(ECC)^2}. \quad (13)$$

Fig. 10, *b* shows that the fabricated antenna has ECC and DG of about 0–0.001 dB and 9.99–10 dB in the resonant frequency range of 2.5–4.5 GHz. This finding indicates that the proposed antenna has high independence and diversity. Additionally, high diversity gain contributes to better data throughput and coverage, making the antenna system more efficient in delivering consistent performance in challenging conditions, such as urban environments or areas with obstacles.

To validate the independence and mutual coupling of the proposed antenna, a comprehensive observation of the electric field concentration by EM simulation is proposed as shown in Fig. 11, *a*. The electric field of the proposed antenna is observed at a resonant frequency of 3.5 GHz and shows that the resulting mutual coupling is low as indicated by the highest electric field only at the antenna at port 1 (P1) and does not distribute the electric field to the antenna at port 2 (P2).

Furthermore, the beamforming of the proposed antenna is shown in Fig. 11, *b* where the main lobe radiates electromagnetic waves to the front of the antenna while the side lobes radiate to the top, bottom and back of the antenna. Furthermore, the radiation pattern of the simulation and measurement process illustrated in Fig. 11, *c* shows a straight and similar result where the maximum radiation is at an angle of 0 with a transmit power of about 17.8 dB. This finding indicates that the proposed antenna has operated optimally at a resonance frequency of 3.5 GHz and supports MIMO for 5G communication systems. Moreover, a comparison of bandwidth and gain for the development models of the proposed antenna is shown in Tables 1, 2.

The bandwidth and gain enhancement of the antenna can be determined using the following equation:

$$BW = \frac{(Optimized\ BW - Initial\ BW)}{Initial\ BW} \times 100\,\%, \quad (14)$$

$$Gain = \frac{(Optimized\ Gain - Initial\ Gain)}{Initial\ Gain} \times 100\,\%. \quad (15)$$

Table 1

Comparison of bandwidth for the proposed antenna models

Model	Frequency range (GHz)	Bandwidth (MHz)
1st model	3.48–3.52	40
2nd model	3.2–3.6	400
3rd model	3.3–3.6	300
4th model	3.3–3.6	300
5th model	3–3.6	600
6th model	3–3.65	650

Table 2

Comparison of gain for the proposed antenna models

Model	Frequency range (GHz)	Gain (dB)
1st model	3.48–3.52	5.8
2nd model	3.2–3.6	7.82
3rd model	3.3–3.6	9.9
4th model	3.3–3.6	10.8
5th model	3–3.6	16.09
6th model	3–3.65	17.8

Based on equation (14) and equation (15), the increase in gain and bandwidth is obtained by calculating the difference between the bandwidth and gain of the antenna with the initial condition and the optimized condition. In this study, the initial bandwidth and gain used are single-element antennas while the bandwidth and optimization gain are obtained from MIMO array antennas with 8×2 elements.

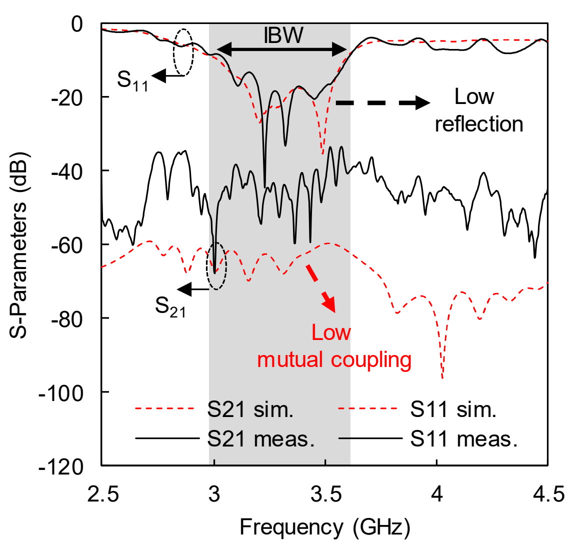

a

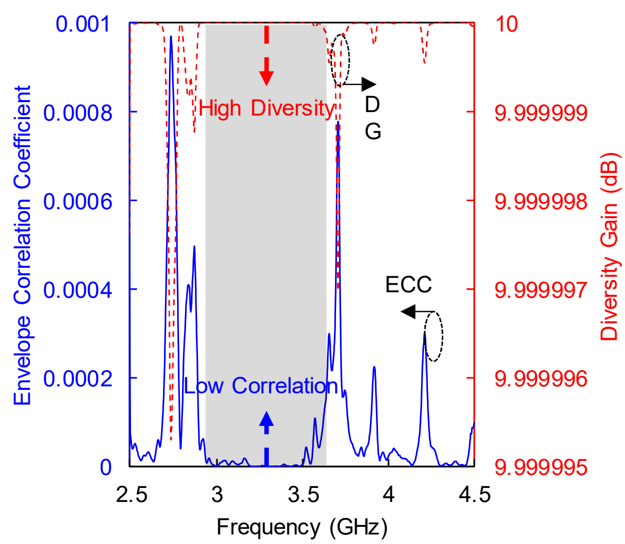

b

Fig. 10. Performance of the proposed antenna: *a* — comparison of the simulation and measurement results of S_{11} and S_{21}; *b* — envelope correlation coefficient and diversity gain based on measurement results

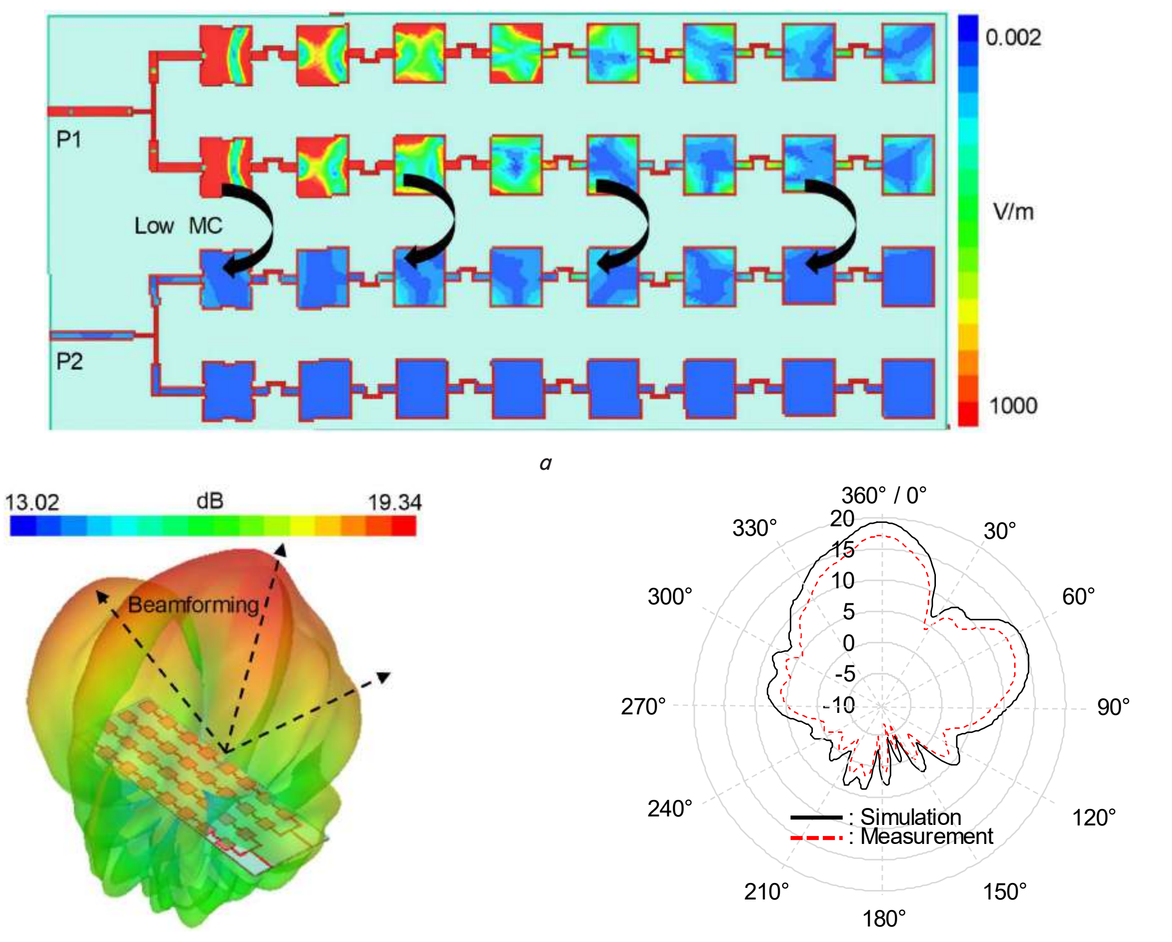

Fig. 11. MIMO performance of the proposed antenna: *a* – simulation of the E-field concentration of the proposed antenna at f_r=3.5 GHz; *b* – 3D simulation of the radiation of the proposed antenna at f_r=3.5 GHz; *c* – comparison of the simulation and measurement of the radiation pattern at f_r=3.5 GHz

6. Discussion of performance validation of the proposed MIMO antenna

Based on the measurement process, the comparison of the bandwidth of all the proposed antenna models is shown in Table 1. Based on Table 1, the bandwidth of the antenna with model 1 increases significantly from 40 MHz to 400 MHz in model 2 and 300 MHz in models 3 and 4. Furthermore, in models 5 and 6, the bandwidth increases to 600 MHz and 650 MHz. From the measurement results, it is found that the bandwidth of the antenna increases up to 1,525 % compared to the single-element antenna.

Furthermore, evaluation is also done by observing the gain of the proposed antenna. The gain comparison of the entire antenna model is shown in Table 2. Based on Table 2, the antenna gains increase in line with the addition of the number of elements of the antenna array. In model 1, the antenna gain is 5.8 dB while for model 2, model 3 and model 4, the antenna gains increase to 7.8 dB, 9.9 dB and 10.2 dB, respectively. Furthermore, in model 5 and model 6, the antenna gains increase to 16.09 and 17.8 dB.

Overall, the gain of the antenna increases up to 206.8 % compared to the single-element antenna. This finding shows that the evolution of the antenna has successfully improved the antenna performance by producing high gain. In addition, the MIMO performance of the antenna is shown with high mutual coupling $S_{21}\leq-20$ dB. From the measurement results, a mutual coupling S_{21} of –40 dB was obtained in the frequency range of 2.5 4.5 GHz. MIMO performance is also indicated by high diversity with a diversity gain of 9.9 dB and a low correlation of 0.0001. This finding shows that the antennas have high independence and do not affect each other when working together.

From the results obtained, the proposed antenna has a performance with wide bandwidth and high gain compared to previous works [15–18]. In addition, the proposed antenna also has the capability for a high-performance MIMO system compared to the previous work [19], which proposed an antenna for a 5G communication system that does not support MIMO systems.

However, there are certain limitations, such as the relatively large antenna dimensions and its operation being restricted to a single resonant frequency. Consequently, future research efforts will focus on minimizing the antenna's dimensions and enhancing its performance across multiple resonant frequencies, enabling its application in other communication systems like 4G, Zigbee, and Wi-Fi.

7. Conclusions

1. From the measurement results, it was found that the proposed antenna has operated at a frequency of 3.5 GHz

with a wide bandwidth of 680 MHz. The bandwidth of the antenna has successfully met the standard requirements for a 5G communication system where the minimum bandwidth is ≤200 MHz.

2. The gain of the proposed antenna was successfully increased gradually using a series planar array with 8×2 elements. From the measurement results, a gain of 17.8 dB was obtained. This finding indicates that the proposed antenna has met the target with a gain of ≥12 dB for a 5G communication system.

3. The proposed antenna has been successfully developed with a two-port MIMO configuration operating at a resonant frequency of 3.5 GHz. From the measurement results, it was found that the proposed antenna has a high mutual coupling with S_{21} of −40 dB with ECC 0.001 and DG 9.99 dB. This finding indicates that the proposed antenna has met the criteria of high mutual coupling with S_{21}≤−20 dB.

Conflict of interest

The authors declare that they have no conflict of interest in relation to this research, whether financial, personal, authorship or otherwise, that could affect the research, and its results presented in this paper.

Financing

This work is supported by the Research Institute of Universitas Trisakti and the Indonesian Ministry of Research, Technology and Higher Education 2024 through a competitive research grant under the Fundamental Research Scheme, contract number 832/LL3/AL.04/2024 and 181/A/LPPM-P/USAKTI/VI/2024.

Data availability

The manuscript has no associated data.

Use of artificial intelligence

The authors confirm that they did not use artificial intelligence technologies when creating the current work.

References

1. Kamal, S., Bin Ain, M. F., Ullah, U., Mohammed, A. S. B., Najmi, F., Hussin, R. et al. (2021). Wheel-shaped miniature assembly of circularly polarized wideband microstrip antenna for 5G mmWave terminals. Alexandria Engineering Journal, 60 (2), 2457–2470. https://doi.org/10.1016/j.aej.2020.12.054
2. Fante, K. A., Gemeda, M. T. (2021). Broadband microstrip patch antenna at 28 GHz for 5G wireless applications. International Journal of Electrical and Computer Engineering (IJECE), 11 (3), 2238. https://doi.org/10.11591/ijece.v11i3.pp2238-2244
3. Tarpara, N., Rathwa, R. R., Kotak, D. N. A. (2018). Design of Slotted Microstrip patch Antenna for 5G Application. Int. Res. J. Eng. Technol., 5 (4), 2827–2832.
4. Hussain, R., Alreshaid, A. T., Podilchak, S. K., Sharawi, M. S. (2017). Compact 4G MIMO antenna integrated with a 5G array for current and future mobile handsets. IET Microwaves, Antennas & Propagation, 11 (2), 271–279. https://doi.org/10.1049/iet-map.2016.0738
5. Deng, J., Li, J., Zhao, L., Guo, L. (2017). A Dual-Band Inverted-F MIMO Antenna With Enhanced Isolation for WLAN Applications. IEEE Antennas and Wireless Propagation Letters, 16, 2270–2273. https://doi.org/10.1109/lawp.2017.2713986
6. Ojaroudi Parchin, N., Jahanbakhsh Basherlou, H., Al-Yasir, Y. I. A., Ullah, A., Abd-Alhameed, R. A., Noras, J. M. (2019). Multi-Band MIMO Antenna Design with User-Impact Investigation for 4G and 5G Mobile Terminals. Sensors, 19 (3), 456. https://doi.org/10.3390/s19030456
7. Hikmaturokhman, A., Ramli, K., Suryanegara, M. (2018). Spectrum Considerations for 5G in Indonesia. 2018 International Conference on ICT for Rural Development (IC-ICTRuDev). https://doi.org/10.1109/icictr.2018.8706874
8. Hobbs, S. (2018). Valuing 5G Spectrum: Valuing the 3.5 GHz and C-Band Frequency Range. Coleago Consulting.
9. An, W., Li, Y., Fu, H., Ma, J., Chen, W., Feng, B. (2018). Low-Profile and Wideband Microstrip Antenna With Stable Gain for 5G Wireless Applications. IEEE Antennas and Wireless Propagation Letters, 17 (4), 621–624. https://doi.org/10.1109/lawp.2018.2806369
10. Pratiwi, A. R., Setijadi, E., Hendrantoro, G. (2020). Design of Two-Elements Subarray with Parasitic Patch for 5G Application. 2020 International Seminar on Intelligent Technology and Its Applications (ISITIA), 7, 311–316. https://doi.org/10.1109/isitia49792.2020.9163785
11. Tang, X., Jiao, Y., Li, H., Zong, W., Yao, Z., Shan, F. et al. (2019). Ultra-Wideband Patch Antenna for Sub-6 GHz 5G Communications. 2019 International Workshop on Electromagnetics: Applications and Student Innovation Competition (IWEM). https://doi.org/10.1109/iwem.2019.8887933
12. Murugan, S. (2021). Compact MIMO Shorted Microstrip Antenna for 5G Applications. International Journal of Wireless and Microwave Technologies, 11 (1), 22–27. https://doi.org/10.5815/ijwmt.2021.01.03
13. Naik, P. S., Virani, H. G. (2020). 1×4 Microstrip Patch Slotted Array Antenna for 5G C-Band Access Point Application. 2020 International Conference on Electronics and Sustainable Communication Systems (ICESC), 1, 641–644. https://doi.org/10.1109/icesc48915.2020.9156015

14. Aghoutane, B., Das, S., EL Ghzaoui, M., Madhav, B. T. P., El Faylali, H. (2022). A novel dual band high gain 4-port millimeter wave MIMO antenna array for 28/37 GHz 5G applications. AEU - International Journal of Electronics and Communications, 145, 154071. https://doi.org/10.1016/j.aeue.2021.154071
15. Naga Jyothi Sree, G., Nelaturi, S. (2021). Design and experimental verification of fractal based MIMO antenna for lower sub 6-GHz 5G applications. AEU - International Journal of Electronics and Communications, 137, 153797. https://doi.org/10.1016/j.aeue.2021.153797
16. Hu, W., Liu, X., Gao, S., Wen, L.-H., Qian, L., Feng, T. et al. (2019). Dual-Band Ten-Element MIMO Array Based on Dual-Mode IFAs for 5G Terminal Applications. IEEE Access, 7, 178476–178485. https://doi.org/10.1109/access.2019.2958745
17. Xu, K. D., Zhu, J., Liao, S., Xue, Q. (2018). Wideband Patch Antenna Using Multiple Parasitic Patches and Its Array Application With Mutual Coupling Reduction. IEEE Access, 6, 42497–42506. https://doi.org/10.1109/access.2018.2860594
18. Alam, S., Surjati, I., Sari, L., Anindito, A., Putranto, A. Y., Firmansyah, T. (2021). Bandwidth Enhancement of Array Microstrip Antenna Using Spiral Stub For 5G Communication System. PRZEGLĄD ELEKTROTECHNICZNY, 1 (11), 42–46. https://doi.org/10.15199/48.2021.11.07
19. Alam, S., Surjati, I., Sari, L., Ningsih, Y. K., Suryadi, S., Trihantoro, G. et al. (2023). Wide band and high gain microstrip antenna using planar series array 4×2 element for 5G communication system. Eastern-European Journal of Enterprise Technologies, 4 (5 (124)), 16–24. https://doi.org/10.15587/1729-4061.2023.285395
20. Putri, S., Surjati, I., Alam, S., Ningsih, Y. K., Sari, L., Firmansyah, T., Zakaria, Z. (2024). High Isolation of Dual-Band MIMO Microstrip Antenna with Vertical – Horizontal Configuration for 5G Communication System. PRZEGLĄD ELEKTROTECHNICZNY, 1 (4), 89–95. https://doi.org/10.15199/48.2024.04.17
21. Fang, D. G. (2017). Antenna Theory and Microstrip Antennas. CRC Press. https://doi.org/10.1201/b10302
22. Garg, R., Bhartia, P., Bahl, I. J., Ittipiboon, A. (2001). Microstrip antenna design handbook. ARTECH HOUSE. Available at: https://uodiyala.edu.iq/uploads/PDF%20ELIBRARY%20UODIYALA/EL37/Microstrip%20Antenna%20Design%20Handbook.pdf

Eastern-European Journal of Enterprise Technologies

COUNTRY

Ukraine

Universities and research institutions in Ukraine

Media Ranking in Ukraine

SUBJECT AREA AND CATEGORY

Agricultural and Biological Sciences
- Food Science

Business, Management and Accounting
- Management of Technology and Innovation

Computer Science
- Computer Science Applications

Energy
- Energy Engineering and Power Technology

Engineering
- Control and Systems Engineering
- Electrical and Electronic Engineering
- Industrial and Manufacturing Engineering
- Mechanical Engineering

Environmental Science
- Environmental Chemistry

Mathematics
- Applied Mathematics

PUBLISHER

Technology Center

H-INDEX

36

SCOPE

Information not localized

Join the conversation about this journal

Quartiles

FIND SIMILAR JOURNALS

1
EUREKA, Physics and Engineering
EST
30%
similarity

2
Naukovyi Visnyk Natsionalnoho Hirnychoho
UKR
21%
similarity

3
Journal of the Balkan Tribological Association
BGR
19%
similarity

4
Journal of C Technologie
UKR
1
si

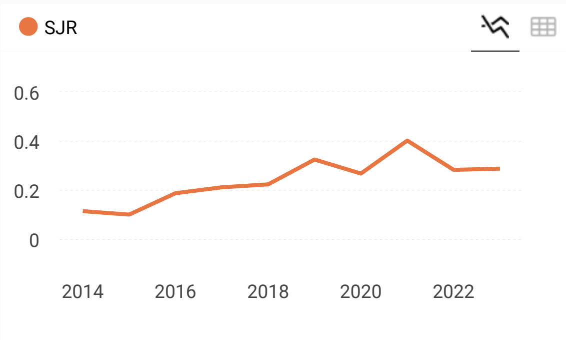

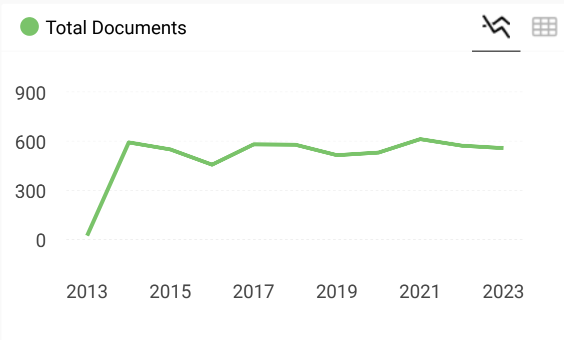

Total Cites Self-Cites

Citations per document

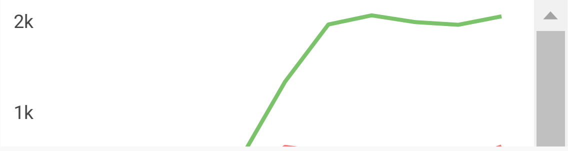

External Cites per Doc Cites per Doc

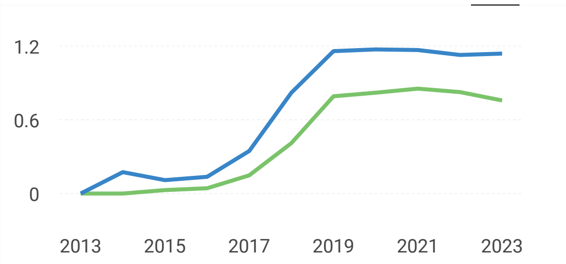

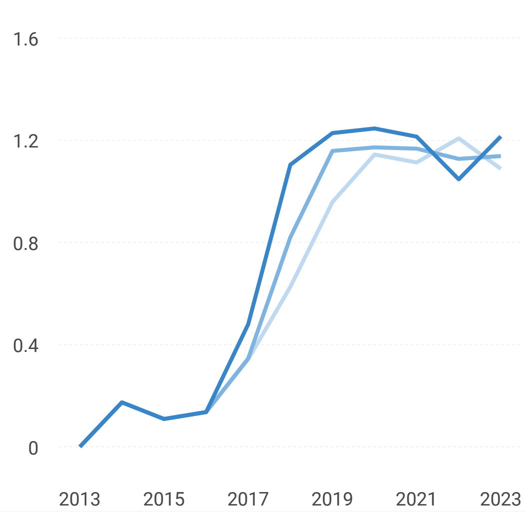

% International Collaboration

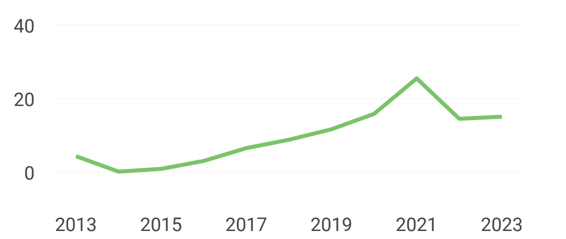

Citable documents Non-citable documents

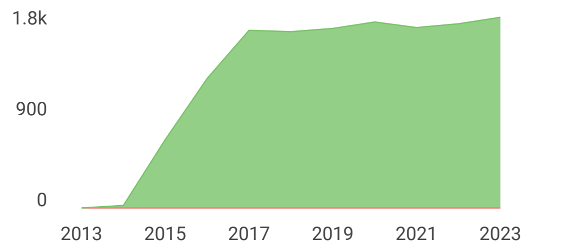

Cited documents Uncited documents

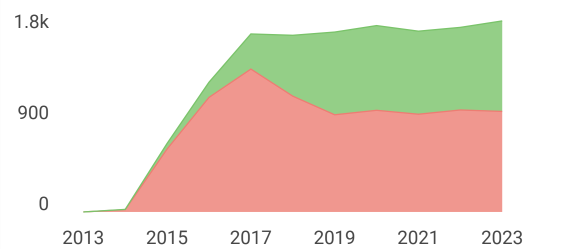

% Female Authors

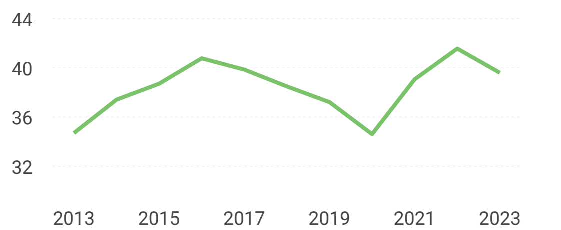

Documents cited by public policy (Overton)

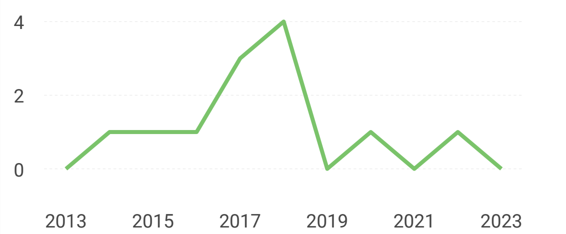

Documents related to SDGs (UN)

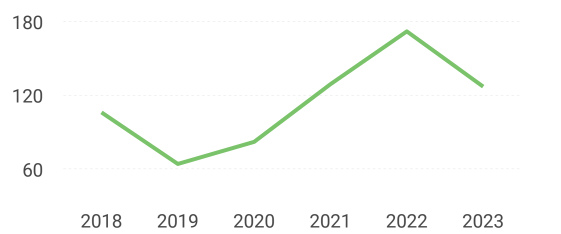

Show this widget in your own website

Just copy the code below and paste within your html code:

<a href="https://www.scimag

Metrics based on Scopus® data as of March 2024

Loading comments...

This author profile is generated by Scopus. Learn more

Alam, Syah

Universitas Trisakti, Jakarta, Indonesia   57191903622
https://orcid.org/0000-0002-0162-8364   View more

223	61	9	View more metrics
Citations by ***166 documents***	Documents	*h*-index View *h*-graph	

Document & citation trends

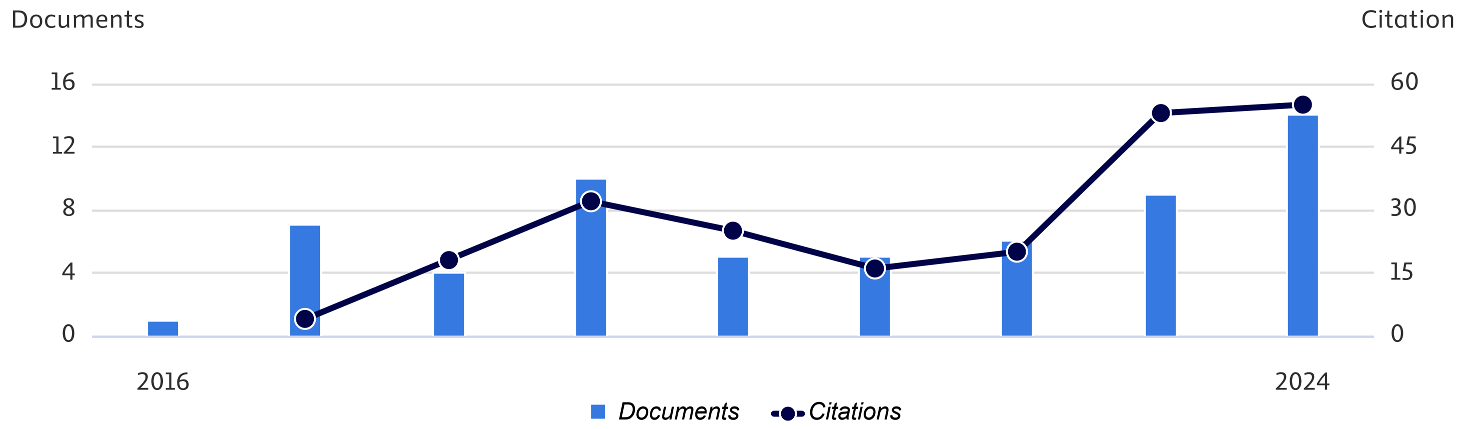

Analyze author output   Citation overview

Most contributed Topics 2019–2023

Antenna Arrays; Resonator; Dielectrics

17 documents

Resonator; Microwave Sensor; Permittivity

7 documents

Antenna Arrays; Output System; Multiple-Input Multiple-Output

2 documents

View all Topics

61 Documents   New Impact   Cited by 166 documents Beta   1 Preprint   89 Co-Authors

12 Topics   0 Awarded Grants

61 documents Alam, Syah

Export all Save all to list Sort by Date (newest)

Article

PERFORMANCE ANALYSIS OF LT-BCH CODE FOR WIRELESS BODY AREA NETWORK

Sari, L., Alam, S., Surjati, I.

Journal of Theoretical and Applied Information Technology, 2024, 102(20), pp. 7440–7448

Show abstract Related documents

0 Citations

Article • *Open access*

Effects of Number of Filters and Frequency Cutoff in Continuous Interleaved Sampling and Frequency Amplitude Modulation Encoding Schemes in Cochlear Implant

Sari, L., Naud, M., Alam, S., Surjati, I.

International Journal of Electrical and Electronics Research, 2024, 12(3), pp. 1010–1017

Show abstract View at Publisher Related documents

0 Citations

Article

Collaboratively Far-Field and Near-Field Regions for Dual-Modalities Microwave Permittivity Sensor Using T-Shaped Resonator Embedded With IDC

Alam, S., Zakaria, Z., Surjati, I., ... Ningsih, Y.K., Sari, L.

IEEE Sensors Letters, 2024, 8(7), 3501304

Show abstract View at Publisher Related documents

0 Citations

Article

Integrated and Independent Solid Microwave Sensor with Dual-Band Bandpass Filter Through Unified Mux-Demux Structure

Firmansyah, T., Praptodiyono, S., Muttakin, I., ... Alaydrus, M., Kondoh, J.

IEEE Sensors Journal, 2024, 24(12), pp. 19253–19261

Show abstract View at Publisher Related documents

1 Citations

Article

Multifunctional Glass Microfluidic Microwave Sensor Attenuator for Detection of Permittivity and Conductivity With Device Protection

Firmansyah, T., Praptodiyono, S., Muttakin, I., ... Wibisono, G., Kondoh, J.

IEEE Sensors Journal, 2024, 24(4), pp. 4574–4585

Show abstract View at Publisher Related documents

1 Citations

Article

Eliminating Dispersion Power Fading in Radio over Fiber Communication through Unbalanced Sideband Modulation

Alam, Syah

Ujang, F., Anhar, Butar, E.E.B., ... Alfanz, R., Firmansyah, T.

International Journal of Electrical and Electronic Engineering and Telecommunications, 2024, 13(6), pp. 456–466

Show abstract View at Publisher Related documents

Article • *Open access*

DEVELOPMENT MODEL OF A HIGH-PERFORMANCE MULTIPLE INPUT MULTIPLE OUTPUT MICROSTRIP ANTENNA BASED ON A PLANAR SERIES ARRAY WITH 8×2 ELEMENTS FOR 5G COMMUNICATION SYSTEMS

Alam, S., Surjati, I., Sari, L., ... Firmansyah, T., Zakaria, Z.

Eastern-European Journal of Enterprise Technologies, 2024, 5(5(131)), pp. 37–49

Show abstract View at Publisher Related documents

Article • *Open access*

Bandwidth enhancement of circular structure microstrip antenna based on inverted C-shaped ground configuration

Wardoyo, S., Permana, J., Supriyanto, T., ... Alam, S., Firmansyah, T.

International Journal of Electronics and Telecommunications, 2024, 70(3), pp. 655–660

Show abstract View at Publisher Related documents

Article

Analysis of Leaf Moisture of Chinese Mustard Green and Water Spinach using Single-Port Circular SRR Microwave Sensor for Post-Harvest in the Agriculture Industry | Analiza wilgotności liści gorczycy chińskiej i szpinaku wodnego przy użyciu jednoportowego okrągłego czujnika mikrofalowego SRR do stosowania po zbiorach w przemyśle rolniczym

Al Subramaniam, S.A., Shairi, N.A., Zakaria, Z., ... Zahari, M.K., Alam, S.

Przeglad Elektrotechniczny, 2024, (8), pp. 251–254

Show abstract View at Publisher Related documents

Article • *Open access*

Dual Functional Liquid Displacement and Angular Detection Based on Band Stop Response Microwave Sensor

Alam, S., Surjati, I., Sari, L., ... Alaydrus, M., Rahayu, Y.

IEEE Access, 2024, 12, pp. 94861–94869

Show abstract View at Publisher Related documents

Author Position

Alam, Syah

Based on 46 selected documents for 2014 - 2023

First author 54%

25	4	0.736
Documents	Average citations	FWCI

Last author 20%

Co-author 26%

Single author 0%

View author position details

View more metrics

View list in search results format

View references

Set document alert

SYAH ALAM

Universitas Trisakti
S2 - Teknik Elektro
SINTA ID : 257111

Microstrip Antenna | Wireless Communication | Telecommunication | Microwave Sensor

2.465
SINTA Score Overall

728
SINTA Score 3Yr

2.465
Affil Score

728
Affil Score 3Yr

Articles | Researches | Community Services | IPRs | Books | PAK | Expertise | Metrics

Latest number of publications

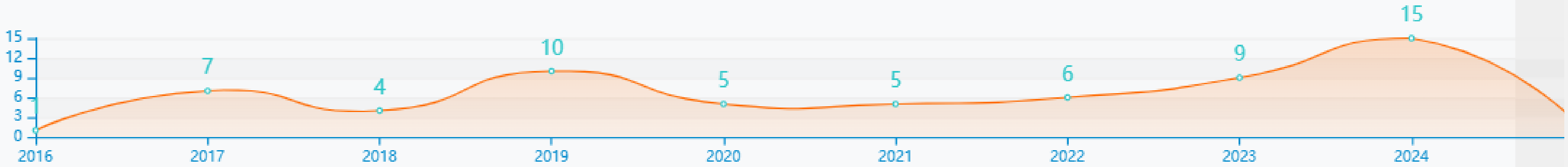

Scopus | Garuda | Google Scholar | RAMA

Search...

Scopus Analysis

[Eliminating Dispersion Power Fading in Radio over Fiber Communication through Unbalanced Sideband Modulation]

Q2 as Journal | International Journal of Electrical and Electronic Engineering and Telecommunications

Author Order : 5 of 8 | Creator : Ujang F.

2024 | 0 cited

[Bandwidth enhancement of circular structure microstrip antenna based on inverted C-shaped ground configuration]

Q3 as Journal | International Journal of Electronics and Telecommunications

Author Order : 0 of 7 | Creator : Wardoyo S.

2024 | 0 cited

[DEVELOPMENT MODEL OF A HIGH-PERFORMANCE MULTIPLE INPUT MULTIPLE OUTPUT MICROSTRIP ANTENNA BASED ON A PLANAR SERIES ARRAY WITH 8×2 ELEMENTS FOR 5G COMMUNICATION SYSTEMS]

Q3 as Journal | Eastern-European Journal of Enterprise Technologies

Author Order : 1 of 7 | Creator : Alam S.

2024 | 0 cited

[Effects of Number of Filters and Frequency Cutoff in Continuous Interleaved Sampling and Frequency Amplitude Modulation Encoding Schemes in Cochlear Implant]

Q3 as Journal International Journal of Electrical and Electronics Research

Author Order : 3 of 4 Creator : Sari L.

2024 0 cited

Analysis of Leaf Moisture of Chinese Mustard Green and Water Spinach using Single-Port Circular SRR Microwave Sensor for Post-Harvest in the Agriculture Industry

Q4 as Journal Przeglad Elektrotechniczny

Author Order : 6 of 6 Creator : Al Subramaniam S.A.

2024 0 cited

Bandwidth enhancement for QMSIW antenna by using dual cavity and triangle slot

Q3 as Journal International Journal of Electronics and Telecommunications

Author Order : 7 of 8 Creator : Astuti D.W.

2024 0 cited

Dual-Band MIMO Circular Patch Microstrip Antenna (CPMA) with Low Mutual Coupling for 5G Communication System

Q3 as Journal Journal of Nano- and Electronic Physics

Author Order : 3 of 8 Creator : Putri S.M.

2023 1 cited

Independent Permittivity Sensor Based on Dual T-Shaped Resonator for Solid Material Characterization

no-Q as Conference Proceedin 2023 IEEE International Symposium on Antennas and Propagation, ISAP 2023

Author Order : 1 of 6 Creator : Alam S.

2023 0 cited

COMPARISON PERFORMANCE ANALYSIS OF ATTENDANCE SYSTEM IN LOS AND NLOS CONDITIONS USING LORA, FSK, AND OOK MODULATION

Q3 as Journal Journal of Engineering Science and Technology

Author Order : 3 of 3 Creator : Rahayu Y.

2023 0 cited

WIDE BAND AND HIGH GAIN MICROSTRIP ANTENNA USING PLANAR SERIES ARRAY 4x2 ELEMENT FOR 5G COMMUNICATION SYSTEM

Q3 as Journal Eastern-European Journal of Enterprise Technologies

Author Order : 1 of 8 Creator : Alam S.

2023 1 cited

Previous 1 2 3 4 5 Next

Page 2 of 7 | Total Records 63

Get More with SINTA Insight

Go to Insight

INDRA SURJATI

Universitas Trisakti
Profesi - Program Profesi Insinyur
SINTA ID : 5984150

Microstrip

2.167
SINTA Score Overall

454
SINTA Score 3Yr

2.167
Affil Score

454
Affil Score 3Yr

Articles Researches Community Services IPRs Books PAK Expertise Metrics

Latest number of publications

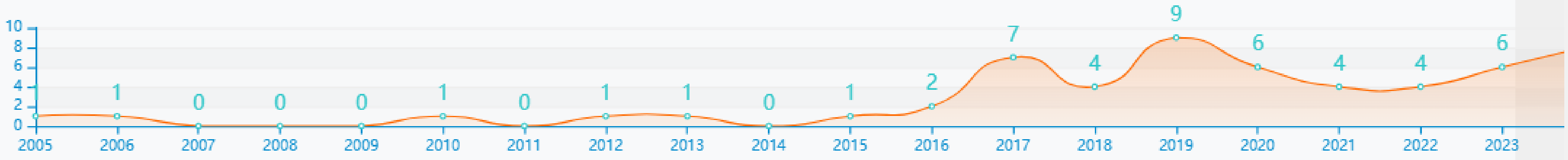

Scopus Garuda Google Scholar RAMA

Search...

Scopus Analysis

DEVELOPMENT MODEL OF A HIGH-PERFORMANCE MULTIPLE INPUT MULTIPLE OUTPUT MICROSTRIP ANTENNA BASED ON A PLANAR SERIES ARRAY WITH 8×2 ELEMENTS FOR 5G COMMUNICATION SYSTEMS
Q3 as Journal Eastern-European Journal of Enterprise Technologies
Author Order : 2 of 7 Creator : Alam S.
2024 0 cited

Effects of Number of Filters and Frequency Cutoff in Continuous Interleaved Sampling and Frequency Amplitude Modulation Encoding Schemes in Cochlear Implant
Q3 as Journal International Journal of Electrical and Electronics Research
Author Order : 4 of 4 Creator : Sari L.
2024 0 cited

PERFORMANCE ANALYSIS OF LT-BCH CODE FOR WIRELESS BODY AREA NETWORK
Q4 as Journal Journal of Theoretical and Applied Information Technology
Author Order : 3 of 3 Creator : Sari L.
2024 0 cited

UHF-Band Solid Sensor Based on Tweaking Electric Field Coupled Resonator for Material Characterization

Q3 as Journal Progress In Electromagnetics Research M

Author Order : 2 of 9 Creator : Alam S.

2024 0 cited

High Isolation of Dual-Band MIMO Microstrip Antenna with Vertical – Horizontal Configuration for 5G Communication System

Q4 as Journal Przeglad Elektrotechniczny

Author Order : 2 of 7 Creator : Putri S.M.

2024 1 cited

Dual-Band MIMO Circular Patch Microstrip Antenna (CPMA) with Low Mutual Coupling for 5G Communication System

Q3 as Journal Journal of Nano- and Electronic Physics

Author Order : 1 of 8 Creator : Surjati I.

2024 0 cited

Dual Functional Liquid Displacement and Angular Detection Based on Band Stop Response Microwave Sensor

Q1 as Journal IEEE Access

Author Order : 2 of 9 Creator : Alam S.

2024 0 cited

Collaboratively Far-Field and Near-Field Regions for Dual-Modalities Microwave Permittivity Sensor Using T-Shaped Resonator Embedded With IDC

Q2 as Journal IEEE Sensors Letters

Author Order : 3 of 8 Creator : Alam S.

2024 0 cited

Independent Permittivity Sensor Based on Dual T-Shaped Resonator for Solid Material Characterization

no-Q as Conference Proceedin 2023 IEEE International Symposium on Antennas and Propagation, ISAP 2023

Author Order : 5 of 6 Creator : Alam S.

2023 0 cited

Highly Independent Dual-Band Permittivity Sensors for Simultaneous Measurement of Solid Materials

no-Q as Conference Proceedin 2023 33rd International Conference Radioelektronika, RADIOELEKTRONIKA 2023

Author Order : 3 of 6 Creator : Alam S.

2023 0 cited

Previous 1 2 3 4 5 Next

Page 1 of 6 | Total Records 56

LYDIA SARI

Universitas Trisakti
S2 - Teknik Elektro
SINTA ID : 5980733

Wireless telecommunication | Information Theory

897
SINTA Score Overall

263
SINTA Score 3Yr

897
Affil Score

263
Affil Score 3Yr

Articles | Researches | Community Services | IPRs | Books | PAK | Expertise | Metrics

Latest number of publications

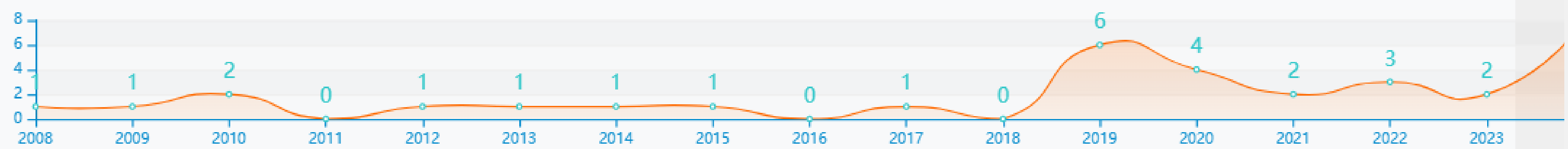

Scopus | Garuda | Google Scholar | RAMA

Search...

Scopus Analysis

PERFORMANCE ANALYSIS OF LT-BCH CODE FOR WIRELESS BODY AREA NETWORK
Q4 as Journal | Journal of Theoretical and Applied Information Technology
Author Order : 0 of 3 | Creator : Sari L.
2024 | 0 cited

UHF-Band Solid Sensor Based on Tweaking Electric Field Coupled Resonator for Material Characterization
Q3 as Journal | Progress In Electromagnetics Research M
Author Order : 0 of 9 | Creator : Alam S.
2024 | 0 cited

High Isolation of Dual-Band MIMO Microstrip Antenna with Vertical – Horizontal Configuration for 5G Communication System
Q4 as Journal | Przeglad Elektrotechniczny
Author Order : 0 of 7 | Creator : Putri S.M.
2024 | 1 cited

Dual-Band MIMO Circular Patch Microstrip Antenna (CPMA) with Low Mutual Coupling for 5G Communication System

Q3 as Journal Journal of Nano- and Electronic Physics
Author Order : 0 of 8 Creator : Surjati I.
2024 0 cited

Dual Functional Liquid Displacement and Angular Detection Based on Band Stop Response Microwave Sensor
Q1 as Journal IEEE Access
Author Order : 0 of 9 Creator : Alam S.
2024 0 cited

DEVELOPMENT MODEL OF A HIGH-PERFORMANCE MULTIPLE INPUT MULTIPLE OUTPUT MICROSTRIP ANTENNA BASED ON A PLANAR SERIES ARRAY WITH 8×2 ELEMENTS FOR 5G COMMUNICATION SYSTEMS
Q3 as Journal Eastern-European Journal of Enterprise Technologies
Author Order : 0 of 7 Creator : Alam S.
2024 0 cited

Collaboratively Far-Field and Near-Field Regions for Dual-Modalities Microwave Permittivity Sensor Using T-Shaped Resonator Embedded With IDC
Q2 as Journal IEEE Sensors Letters
Author Order : 0 of 8 Creator : Alam S.
2024 0 cited

Effects of Number of Filters and Frequency Cutoff in Continuous Interleaved Sampling and Frequency Amplitude Modulation Encoding Schemes in Cochlear Implant
Q3 as Journal International Journal of Electrical and Electronics Research
Author Order : 0 of 4 Creator : Sari L.
2024 0 cited

Dual-Band MIMO Circular Patch Microstrip Antenna (CPMA) with Low Mutual Coupling for 5G Communication System
Q3 as Journal Journal of Nano- and Electronic Physics
Author Order : 0 of 8 Creator : Putri S.M.
2023 1 cited

WIDE BAND AND HIGH GAIN MICROSTRIP ANTENNA USING PLANAR SERIES ARRAY 4x2 ELEMENT FOR 5G COMMUNICATION SYSTEM
Q3 as Journal Eastern-European Journal of Enterprise Technologies
Author Order : 0 of 8 Creator : Alam S.
2023 1 cited

Previous 1 2 3 4 Next
Page 1 of 4 | Total Records 34

YULI KURNIA NINGSIH

Universitas Trisakti
Profesi - Program Profesi Insinyur
SINTA ID : 5984592

Telekomunikasi antena microwave

793
SINTA Score Overall

163
SINTA Score 3Yr

793
Affil Score

163
Affil Score 3Yr

Articles Researches Community Services IPRs Books PAK Expertise Metrics

Latest number of publications

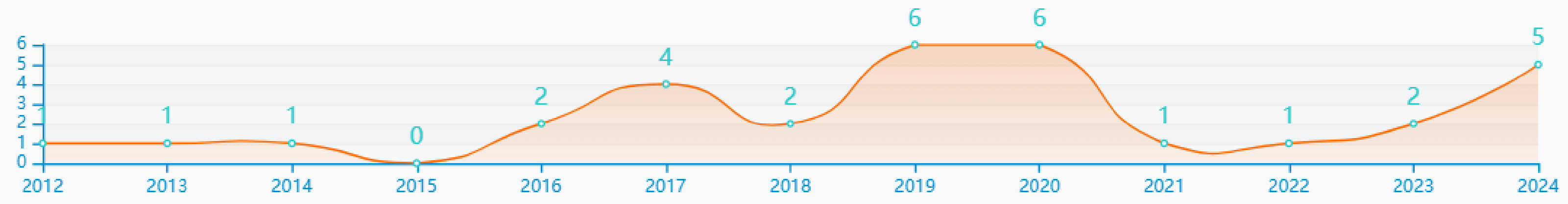

Scopus Garuda Google Scholar RAMA

Search...

Scopus Analysis

DEVELOPMENT MODEL OF A HIGH-PERFORMANCE MULTIPLE INPUT MULTIPLE OUTPUT MICROSTRIP ANTENNA BASED ON A PLANAR SERIES ARRAY WITH 8×2 ELEMENTS FOR 5G COMMUNICATION SYSTEMS
Q3 as Journal Eastern-European Journal of Enterprise Technologies
Author Order : 4 of 7 Creator : Alam S.
2024 0 cited

UHF-Band Solid Sensor Based on Tweaking Electric Field Coupled Resonator for Material Characterization
Q3 as Journal Progress In Electromagnetics Research M
Author Order : 4 of 9 Creator : Alam S.
2024 0 cited

High Isolation of Dual-Band MIMO Microstrip Antenna with Vertical – Horizontal Configuration for 5G Communication System
Q4 as Journal Przeglad Elektrotechniczny
Author Order : 4 of 7 Creator : Putri S.M.
2024 1 cited

Dual-Band MIMO Circular Patch Microstrip Antenna (CPMA) with Low Mutual Coupling for 5G Communication System

Q3 as Journal Journal of Nano- and Electronic Physics
Author Order : 4 of 8 Creator : Surjati I.
2024 0 cited

[Collaboratively Far-Field and Near-Field Regions for Dual-Modalities Microwave Permittivity Sensor Using T-Shaped Resonator Embedded With IDC]
Q2 as Journal IEEE Sensors Letters
Author Order : 7 of 8 Creator : Alam S.
2024 0 cited

[Dual-Band MIMO Circular Patch Microstrip Antenna (CPMA) with Low Mutual Coupling for 5G Communication System]
Q3 as Journal Journal of Nano- and Electronic Physics
Author Order : 5 of 8 Creator : Putri S.M.
2023 1 cited

[WIDE BAND AND HIGH GAIN MICROSTRIP ANTENNA USING PLANAR SERIES ARRAY 4x2 ELEMENT FOR 5G COMMUNICATION SYSTEM]
Q3 as Journal Eastern-European Journal of Enterprise Technologies
Author Order : 4 of 8 Creator : Alam S.
2023 1 cited

[Bandwidth Enhancement and Circular Polarization Microstrip Antenna Using L Slot and Rectangular Parasitic Stacked]
Q3 as Journal Journal of Nano- and Electronic Physics
Author Order : 4 of 8 Creator : Alam S.
2022 0 cited

[Reinforcement learning-based adaptive modulation for vehicular communication]
no-Q as Conference Proceedin ECTI-CON 2021 - 2021 18th International Conference on Electrical Engineering/Electronics, Computer,
Author Order : 2 of 2 Creator : Kurniawati N.
2021 2 cited

[Design of Circular Polarization Microstrip Antenna with Array 4×4 Elements for Microwave Radio]
no-Q as Conference Proceedin 6th International Conference on Computing, Engineering, and Design, ICCED 2020
Author Order : 3 of 6 Creator : Alam S.
2020 0 cited

Previous 1 2 3 4 Next

Page 1 of 4 | Total Records 32

Get More with SINTA Insight

Go to Insight